International Journal of Microwave and Wireless Technologies

cambridge.org/mrf

Broadband millimeter-wave absorbers: a review

Anupriya Choudhary[1], Srikanta Pal[1] and Gautam Sarkhel[2]

[1]Department of Electronics & Communications, Birla Institute of Technology, Mesra, Ranchi 835215, India and [2]Department of Chemical Engineering, Birla Institute of Technology, Mesra, Ranchi 835215, India

Review Paper

Cite this article: Choudhary A, Pal S, Sarkhel G (2023). Broadband millimeter-wave absorbers: a review. *International Journal of Microwave and Wireless Technologies* **15**, 347–363. https://doi.org/10.1017/S1759078722000162

Received: 14 April 2021
Revised: 17 January 2022
Accepted: 18 January 2022
First published online: 15 February 2022

Key words:
Carbon nanotubes; FSS; graphene; metamaterials; millimeter-wave absorbers; polymers

Author for correspondence:
Anupriya Choudhary,
E-mail: anupriya010229@gmail.com

Abstract

This paper reports an exhaustive review of recent research progress in the development of millimeter-wave absorbers. With the advancement in technologies, microwave absorbers have shown their evolution in several applications such as defense, security identification, stealth technology, and several more. The importance of these absorbers is increasing due to electromagnetic interference (EMI) effects. Primarily, an abundant amount of absorbers has been developed in lower frequency bands and with the increasing demand for 5G technology, the usage of millimeter-wave bands has gained attention. This in turn requires the development of millimeter-wave absorbers to provide EMI shielding in several applications. Out of several materials, polymers have grabbed attention in the mitigation of EMI. An absorber that combines carbonaceous elements with polymers offers large design flexibility and tunability per the filler concentration. This paper focuses on the classification of these absorbers based on geometry as well as that by using polymers with their design challenges, merits, and demerits with their industrial applications. Comparative studies of geometrically based absorbers and polymeric-based absorbers are also shown.

Introduction

The modern advancement of wireless communication has induced contamination of the environment due to electromagnetic interference (EMI). Out of all the known sources of pollution, electromagnetic (EM) pollution has turned the table and increased fourfold. Currently, the pollution due to EM radiation is one of the largest growing factors in degrading the environment. It not only harms human beings, but it is extremely harmful to animals and their entire biological life. To reduce the harmful effects of EM radiation, several important innovations have been successful in suppressing them. Out of these, the use of metamaterials (MMs) has shown positive results in the suppression of EMI. EM MMs are artificially engineered materials that make use of sub-wavelength dielectric or metallic elements, giving rise to exotic properties which are not available in nature [1]. These properties arise due to the structural features rather than material constituents. The structural parameters such as size, shape, and geometry can be adjusted to obtain tunable permittivity and permeability values of the MM structure. These MMs have exhibited quite unusual properties such as left-handed behavior, near-zero permittivity, permeability, double-zero behavior, negative refractive index, etc. [2]. These MMs have shown applications in various multiple disciplines such as EMs, optoelectronics, biomedical devices, ranging from low microwave to visible frequency [3]. The most popular applications of MMs are that of the development and design of EM absorbers. The properties of MMs can be achieved by suitably designing these absorbers, along with perfect absorption, which is our main aim in suppressing EMI.

Microwave absorber (MA) materials are used to reduce EMI and enhance the isolation among devices. MAs are used to reduce the amount of energy present in the microwave signal. The structure of an MA consists of unit cells arranged periodically. The top layer consists of a conducting layer with the bottom layer used as the ground plane and a dielectric layer in between both the layers. The principle of absorption primarily deals with impedance matching using a dielectric layer. Its impedance Z_{in} must match with 377 Ω, i.e. the impedance at free space. This would result in zero reflection coefficient, thus maximum absorption occurs. Thus, the incident wave penetrates the dielectric layer. In MAs, since the top layer is conducting, its surface charges get energized with the electric field, which results in a magnetic response, thus causing absorption at the resonant frequency. The current which is generated is circulating as well as parallel, which further induces magnetic and electric responses, respectively. The strong coupling between the electric and magnetic responses gives rise to this current. They couple with the EM wave and very strong electric and magnetic resonances appear at this resonant frequency, thus providing very good EM wave absorption under the matching condition [4]. Mostly in the practical implementations, the cause of EMI is unspecified, as in it may occur due to several sources, at different frequencies, and of unknown polarization. Achieving perfect absorption, at a very

© The Author(s), 2022. Published by Cambridge University Press in association with the European Microwave Association

high frequency, often suffers from one or more properties being forfeited. Attaining high bandwidth, with thickness in nanometers and absorption rate of above 90% is difficult, but has been developed to some extent in the recent past. The absorbers which operate in the frequency range of 30–300 GHz are known as millimeter-wave absorbers. In the past, research study has been carried out to design absorbers with suitable materials and structural features, which could help in obtaining large absorptivity. As the research demand grows in this field, there is a quest for the search of novel materials and designs.

The utilization of polymeric composites and ceramics for the designing of absorbers has been a very important area of research in this field. Traditionally, these are composed of magnetic loss materials, such as magnetic metals [5, 6], ferrites [7, 8], dielectric loss materials that are composed of materials containing carbon, either carbon fibers [9], carbon nanotubes (CNTs) [10, 11], or silica carbide fibers [12], and conducting polymers [13]. Out of all the above carbonaceous materials, a CNT has been a widely used material due to its extensive properties and high conductivity [10–15]. CNTs usually have weak microwave absorption property, so it is combined with other lossy materials to achieve the desired absorptivity [16]. For example, as in the case of ZnO@CNT [17], CdS–MWCNTs [18], CNT@Fe_3O_4 [19], and γ-FeNi/CNT [20]. The two-dimensional (2D), sp^2-hybridized carbon atoms, called graphene, have also shown exceptionally good electrical, thermal, and mechanical properties and are a perfect candidate for microwave absorption. It is capable of dissipation and absorption of EM waves by transforming them into thermal energy [21]. In this paper, we will discuss various recently developed millimeter-wave absorbers based on structural features, followed by those using polymeric composites.

A typical MA looks like as shown in Fig. 1. It consists of *i*-layers of dissimilar materials, supported by a perfect electric conductor.

The two main methods for the characterization of EM materials are non-resonant and resonant methods. The non-resonant method of analysis is mainly focused since it determines the response of electric and magnetic behaviors over a large span of frequencies. Here, the properties of materials are calculated by their wave velocities and impedances in the material medium. The EM parameters of the material are calculated by reflection and/or transmission through the boundary between the free space and material. Coaxial lines, dielectric waveguides, hollow metallic waveguides, planar transmission lines, and free space are used as a medium to carry EM waves to the material.

For the reflection method, a single-scattering parameter, S_{11} is analyzed, where the signal is transmitted and received through the incident port, or port 1. The permittivity and permeability can be deduced, which are quantified in terms of the scattering parameters. For the transmission or reflection method, two-port systems are used, where the signal incident can be split into the reflected and transmitted waves. This can be modified analytically into a 2×2 matrix. The schematic sketch of a two-port system for the analysis of the transmission/reflection method is shown in Fig. 2. Here, the *S*-parameters are calculated from Maxwell's equations applied with the boundary conditions for the selected material. The material to be studied is positioned into a transmission line. The *S*-parameter equations are used to calculate the electric field at the interface. The scattering equations consist of variables relating to the permeability, permittivity of the material inserted, length, and the position of reference planes of the sample.

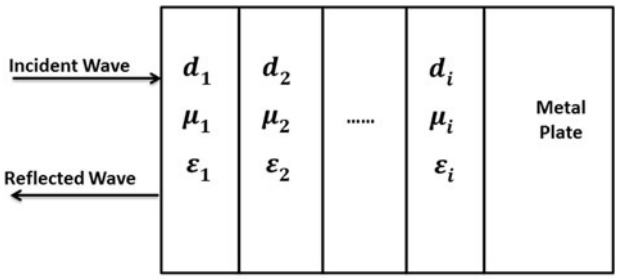


Fig. 1. Schematic representation of a typical *i*-layer MA with thickness, permittivity, and permeability, backed by a metal plate.

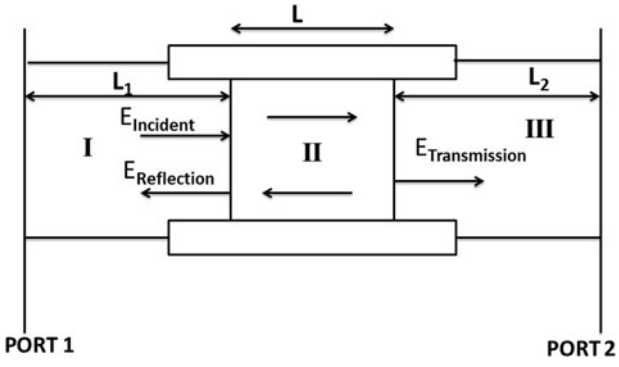


Fig. 2. Schematic representation of a measurement setup for transmission/reflection method.

The primary requirements of an absorber are as follows: (1) it should be able to minimize the reflection at the front surface, (2) impedance matching at the free space to absorber interface must be achieved, (3) the absorber must have large values of dielectric and magnetic losses for EM waves to penetrate, and (4) it does not require an external magnetic field [22]. An absorber with minimal thickness, more particularly in the nanometers range, with high bandwidth and good absorption, are the requirements of 5G technology.

In this paper, we discuss various millimeter-wave broadband absorbers based on structural features and polymeric composites. The design-based challenges are also discussed with various techniques to overcome the same. A comparative analysis of absorptivity for various absorbers is carried out, along with their prospects and applications.

Motivation and outline

In the pursuit of technological advances in the field of communications, we are constantly on the lookout for research interests in the field of EM theory as well as its application in multidisciplinary sectors. The use of polymers in the microwave industry has drawn attention due to its large design flexibility, low cost, ease of fabrication, and ample tunability of the dopant concentration. By controlling the structural parameters as well as the concentration of dopants in polymer composites, the absorption behavior could be enhanced according to the required application. The filler particles in the polymeric composite give rise to polarization phenomena and therefore provide an understanding of the dependence of frequency on the effective permittivity of the material. In what follows, the different types of structures and

https://doi.org/10.1017/S1759078722000162 Published online by Cambridge University Press

polymeric composites to optimize the performance of these millimeter-wave absorbers have been reviewed. To our knowledge, no review has been made in the field of millimeter-wave absorbers based on structure and polymeric composites to date. Although several absorbers have been developed, there are always new objectives to achieve while designing the same, for various applications. Despite the advancement, there are several challenges faced by researchers while developing the same. Some of these challenges are recognized and discussed in this paper. The remaining paper is organized as follows: in Section "Background theory," we have reviewed the background history of EM wave absorbers, followed by design challenges and techniques to overcome the same in Section "Design challenges." Section "Recently developed millimeter-wave absorbers" discusses the recent progress in the development of millimeter-wave absorbers. It is divided into two parts: one, discussing the millimeter-wave absorbers based on designing and simulating using frequency simulators; second, absorbers developed by polymeric synthesis. This section has been divided into single- and multi-layered absorbers sub-sections for the ease of reading. Comparative tables for the geometrically designed absorbers as well as those synthesized using polymers have been provided. Section "Conclusion" discusses the prospects, applications, and is finally concluded.

Background theory

The demonstration of the very first MA was made possible by Landy *et al.* [3]. This gave rise to a new research interest in the field of microwaves and the absorption theory obtained new domains from microwave to higher bands. The easy realization of a design onto a structure with a suitably good absorption has made it the center of attraction for engineers. In most cases, the origin or the cause of EMI is not certain and may occur in a wide range of frequencies with any polarization, occurring from any direction. Absorbers must be ultrathin and polarization-insensitive, thus achieving a suitably perfect absorption. Despite the requirements, it is difficult to achieve all of them simultaneously. In the recent past, technologies have made it possible to implement flexible and tunable resonators. The composite structures are also useful in acquiring broadband resonance which is not possessed by ordinary mediums [23]. Geometrically, absorbers are categorized as resonant and gradient impedance absorbers. Graded absorbers are also called impedance-matching absorbers. In the graded absorbers, the EM waves experience reflection occurring at the air–absorber interface. This reflection is proportional to the magnitude of the impedance of radiation and transmitted medium. Three types of graded absorbers have been prepared in the past, namely pyramidal, tapered, and matching layer absorbers [24].

One of the earliest studies in MAs is that of a Salisbury screen absorber [25]. It has a thin screen separated by a metallic backing with a dielectric placed at a quarter wavelength from the screen. This is because, in the transmission line theory, whenever a load is kept at a quarter wavelength distance from the metal plate, it forms an open circuit at the resistive sheet, resulting in impedance matching due to zero value of reflection. However, the Salisbury screen suffers from bulkiness and narrow absorption bandwidth. To achieve broadband absorption, Jaumann absorbers were proposed, consisting of multiple resistive sheets and dielectrics. However, the thickness is large. A combination of quarter wavelength thick lossy dielectric material having a metallic ground plane is called a Dallenbach absorber. Multiple stacking of layers is required to achieve broadband behavior. Due to the multiple stacking of layers, the thickness is compromised in this case. One type of broadband absorbers uses a frequency selective surface (FSS). It consists of periodic arrangements of conducting patterns onto a dielectric substrate. These absorbers produce exceptional absorption properties and are substantially light weight. Circuit analog absorbers (CAAs) are made of sheets comprising resistive as well as reactive components. They are realized by using a periodic lossy material as the top layer.

It can be thought of as, at the resonant frequency, the gap between the surface and the bottom layer is a quarter-wavelength. At this point, an RLC equivalent circuit of an absorber experiences resonance. Just like a Jaumann absorber, which consists of multiple resistive sheets, a CAA can be prepared from multiple circuit analog sheets too. It provides large bandwidth but the design and fabrication are quite complex in this case.

Metamaterial absorbers (MMAs) are engineered materials and known for their electric permittivity and magnetic permeability. They are not dependent on any particular property of materials; rather they obtain their novel properties from their geometry or design. By scaling the design parameters, the operating frequency range can be changed [4]. The detailed study of the absorbers in the millimeter-wave frequency range is performed in Section "Recently developed millimeter-wave absorbers."

For an absorber prepared from dielectric materials, it is observed that the thickness of the absorber coating is larger as compared to an absorber prepared from a magnetic material. This is because, in pure dielectrics, both parts of the permittivity are very less as compared to that in a magnetic material, which has larger real values of permittivity and permeability. There are no magnetic properties in a dielectric. For hybrid absorbers, the performance is very efficient with less thickness, as it combines the benefits of dielectric and magnetic materials, providing large loss values. Thus, these absorbers are categorized based on geometrical features, materials, and impedance transition. It is demonstrated in Tables 1 and 2.

Design challenges

Bandwidth–thickness

The fascinating properties of MMs have made it easy to increase the absorptivity of an EM absorber. However, the electric and magnetic resonance occurring within the structure could limit the absorption bandwidth. The perfect absorption could be achieved for a thin absorber when the operating bandwidth is not much wide. However, when a large absorption bandwidth is required with minimal thickness, the development of such absorbers becomes difficult. For example, an eight-resistive Jaumann absorber was designed and above 80% absorptivity was found from 2.95 to 35.2 GHz, but the thickness was much larger, 31.4 mm [26]. For a perfect absorption, it is important to keep a check on the optimal thickness of the absorber as well. The bandwidth and thickness always differ from each other. In simple words, it is difficult to obtain large bandwidth with a very small thickness of the absorber. Therefore, the bandwidth–thickness relationship must be optimized to attain perfect absorption.

Using highly absorbent materials [18], including highly lossy materials [27], integrating different resonant units either in the horizontal or vertical direction [28], utilizing lumped circuits [29], use of magnetic substrates [14], anti-reflection coating

https://doi.org/10.1017/S1759078722000162 Published online by Cambridge University Press

Table 1. EM absorbers based on structural features

	Resonant absorbers			Broadband absorbers	
	Advantages	Disadvantages		Advantages	Disadvantages
Salisbury screen	Light weight, simple design fabrication	Narrowband, $\lambda/4$ separation	FSS	Wideband, insensitive to polarization, gives wide angle	Thick, complex designs, bulky
Jaumann layers	Simple design, high bandwidth	Thick, complex design, optimization, and fabrication	MMAs	Thin, insensitive to polarization, large range of angles	Bandwidth is limited
Dallenbach layer	Simple design, easy fabrication	Narrowband, $\lambda/4$ separation	CAAs	Thin, insensitive to polarization, wideband	Very complex design and fabrication

Table 2. Absorbers based on gradual impedance transition and material properties

	Based on gradual impedance transition			Based on material properties	
	Advantages	Disadvantages		Advantages	Disadvantages
Pyramidal	Gives wideband response, large range of angles, very good absorptivity	Bulky, costly, difficult to design and fabricate	Dielectric	Economical, light weight, wideband	The performance is limited to frequencies above 20 GHz
Matching layer	Thin, very good absorptivity	Narrowband, difficult to design and fabricate	Magnetic	Thin, very large magnetic loss, wideband	Costly
Tapered loading	Wideband response, thinner as compared to pyramidal structures	Difficult to fabricate	Magneto-electric	Thinnest among the above two structures, gives the widest bandwidth	Bulky and costly

[30], based on water [31], resistive films [32], use of transparent spacers such as indium tin oxide (ITO) [33–37], FSSs [38–40], polymeric nanocomposites [41–46], etc. are some of the techniques to overcome this challenge.

Multi-layering is one of the most efficient approaches to obtain large working bandwidth, by the combination of multiple-resonant elements with varying resonant frequencies, inside a single multi-layered unit cell [38--47--49]. Within this multi-layered structure, each layer adds to the losses, thereby enhancing the absorption with large bandwidth and reduced overall thickness. It requires careful selection of the design parameters to achieve perfect absorption while maintaining the required criteria. The fabrication process in such structures is usually complex due to the limited space in a single unit cell. Nevertheless, multi-layering provides enhanced absorption by combining the resonance of each layer in the structure.

Water, on the other hand, is less electrically conductive with good absorption properties.

In the case of resistive thin films or sheets such as ITO, parallel and anti-parallel current flow takes place that induces electric and magnetic fields. They couple with the incoming waves and causes strong absorption at the resonant frequency.

Polarization and incidence angles

For effective microwave absorption, despite the wide bandwidth and low thickness, it is also required for an absorber to be insensitive to the orientation and polarization of EM radiation. There have been several cases in the past, where absorbers are sensitive to the orientation and polarization of the radiation. Such problems have been tried to resolve to achieve the perfect absorption. It has been reported earlier that on increasing the working bandwidth and incidence angles, it was difficult to control the geometry of the structure as it had to suffer from bulkiness and complexity. As the incidence angle increases, the magnetic couplings among the layers of the absorbers become weak, due to which the magnetic resonance reduces, and hence the absorption performance is affected.

The EM radiation can be incident on the absorber with any angle and orientation, thus it is important to develop absorbers that would be insensitive to these factors to achieve good absorption. The relations of absorption characteristics with that of polarizations are directly dependent on the impedance matching of the absorber with that of free space. For 100% absorption, the effective permittivity and permeability are equal in magnitude. In the transverse electric (TE) polarization, it is linked with the electric field of the incident EM waves. When the electric field is parallel to the structure of the absorber, electric resonance occurs. The magnetic resonance decreases as the incidence angle increases, thus resulting in a reduced magnetic field component into the substrate material. Due to this imbalance, there is a mismatch of impedance between the free space and absorber. Similarly, in the case of transverse magnetic (TM) polarization, it is linked with the magnetic field of the incident EM waves. The magnetic resonance occurs when the magnetic field is parallel to the structure of the absorber. Here, the electric resonance reduces on increasing the incidence angle, thus resulting in a mismatch of the impedance between the absorber and free space. This gives us an insight that structure could not be insensitive to TE or TM polarization at all incidence angles.

https://doi.org/10.1017/S1759078722000162 Published online by Cambridge University Press

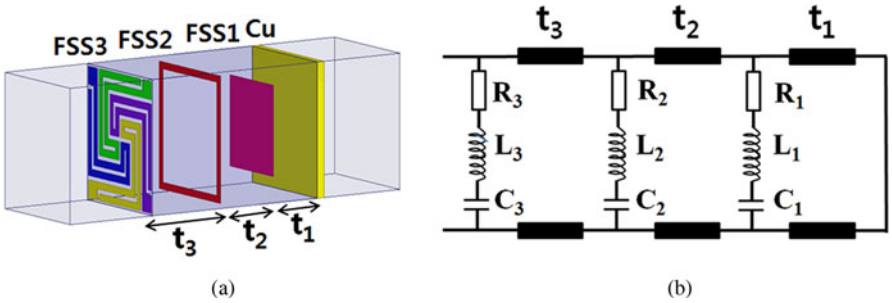


Fig. 3. Illustration of (a) triple-layered FSS absorbers with a combination of FSS1/FSS2/FSS3 (square patch/square loop/spiral) and (b) equivalent circuit. (Reprinted with permission from [55].)

Recently developed millimeter-wave absorbers

Based on structural features

Single-layered absorbers

One of the important methods of increasing the bandwidth of an absorber is by using FSSs with highly absorbing materials [40]. In the past, FSS-based absorbers have shown to be a potential method for good absorption. Despite having good absorptivity, these structures are bulky and fragile. Thickness and bandwidth differences in FSS-based absorbers are the main challenges.

A single-layered FSS absorber was designed by Sakran *et al.* [39] using metallic nichrome circle on a 0.5 mm thick polymethyl-methacrylate (PMMA) substrate. Also, another absorber was prepared from a nichrome circular ring of 0.25 mm thick on an alumina substrate for the W-band, achieving maximum absorptivity at 95 GHz. This was designed for the application of a micro-bolometer array. Here, it was observed that although the ring array had a lower surface coverage than that of the circular one, it still showed better absorption efficiency. However, the circular array gave a broad bandwidth, due to the higher permittivity of the alumina substrate. Jaumann absorbers are broad bandwidth absorbers [50, 51]. But, they suffer from the issue of thickness as compared to Salisbury screens.

To work in 5G, a large bandwidth is required, which can be ensured by using single- and/or dual-band resonators. Embedding of a high-frequency resonator within a low-frequency resonator was carried out to obtain absorptivity at 77, 95, and 110 GHz by Singh *et al.* [52]. The substrate was flexible enough to enhance absorption. Later, they showed that the two resonators placed embedded within one another cause coupling and degrade the performance. By varying the parameters, and bringing the resonance of the second resonator closer to the resonance of the first resonator, the bandwidth, as well as absorption peak, increased. In 2013, the broadband behavior was obtained by embedding one resonator inside another resonator, within each of the unit cells of the absorber lattice. Both the resonators were placed in the same direction to lessen the coupling between them, thus broadening the absorption peak. This absorber was fabricated on a polyimide substrate with gold thin films, in the shape of split-ring resonators which completes the unit cell. This design achieved 98% absorption at 77 GHz, for 8 GHz bandwidth [53].

A flexible MMA was designed by Lee *et al.* [54] with the top layer patterned with silver ink and placed on top of the Kapton polyimide film. The patterning was done via inkjet printing technology. This process is environmentally friendly and does not produce any waste. But, it suffers from difficulty while printing high-resolution patterns at high frequency, since it has low resolution.

Multi-layered absorbers

Multi-layered absorbers are characterized by multiple-resonant layers in a single unit cell. Each of these layers gives different resonant frequencies and producing losses, thereby giving rise to enhanced absorption and broad bandwidth. Recently developed multi-layered MMAs are discussed in this sub-section.

For the millimeter-wave range, an eight-resistive Jaumann absorber was designed and above 80% absorptivity was found for 2.95–35.2 GHz, but the thickness was much larger, 31.4 mm [26]. Narayan *et al.* [38] proposed a cascaded FSS structure prepared from mu-negative (MNG) and double-positive (DPS) layers. This cascading led to absorptivity of more than 95% in 90.4–100 GHz. This structure was prepared without any metal backing for both TE and TM polarization. The number of layers, in this case, was six, out of which, three layers of DPS and MNG were kept alternatively. MNG was prepared from circular split-ring resonators. However, the structure suffered from bulkiness, considering the number of layers.

Multi-layered FSS structures with different patterns of resonant frequencies were used by Liu *et al.* [47]. The equivalent circuit model was used to determine the circuital values of three types of FSS, i.e. square loop, cross, and square patch. The square loop exhibited a low-resonating frequency at 10 GHz due to high values of L and C. However, for the square patch, it was 36 GHz. By tuning the two FSSs, ultra-wide bandwidth from 6.3 to 40 GHz with −10 dB was obtained. The absorber thickness was found to be 5.5 mm. However, the grating lobes increased.

The issue of grating lobes was reduced in [55]. Increasing the periodicity of the unit cell is a simple solution for increasing the lower frequency bound in a multi-layered absorber with the non-magnetic substrate. However, this would reduce the higher frequency bound, which is limited by grating lobes. Therefore, it is important to maintain minimum periodicity with which, large bandwidth could be achieved while reducing grating lobes.

Reducing the size of the unit cell reduces the resonant frequency due to large values of capacitance among the conductors present in the entire circuit. These capacitances add up, thus lowering the resonant frequency and providing ultra-wide bandwidth. For this purpose, a high-capacitive multi-layered FSS with a new structure of folded spiral conductor was designed [55] as shown in Fig. 3. By combining a high-capacitive spiral FSS with other basic FSS structures such as the square loop and square patch, more than 90% absorption for 4.7–50 GHz was achieved. This was tested by free-space measurement of the sample fabricated using the screen printing method, which gave absorption in the bandwidth of 5.2–44 GHz for a thickness of 6.5 mm. For the single-layer FSS absorbers, the substrate was considered as air for simplicity, and reflection loss was measured for each of the absorbers. The S-FSS showed multiple absorption peaks at 6.8, 21.6, 37.8,

https://doi.org/10.1017/S1759078722000162 Published online by Cambridge University Press

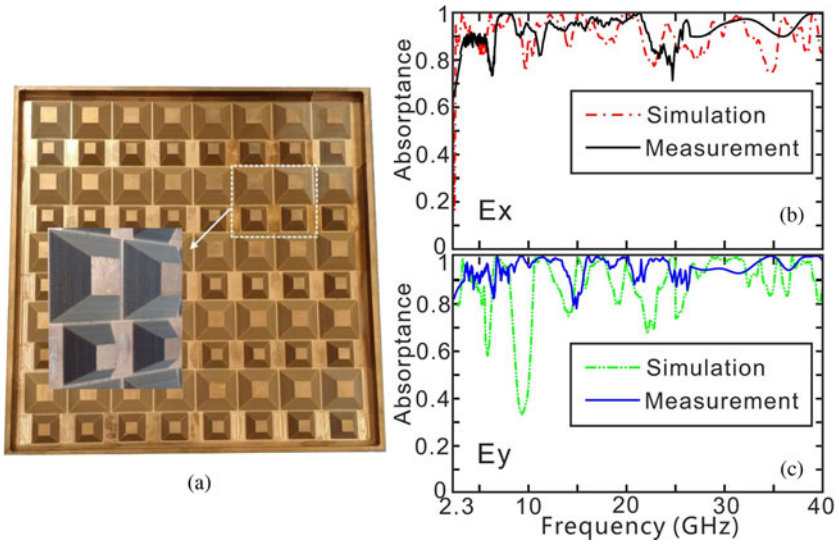


Fig. 4. (a) Fabricated sample of OS-HMM absorber. Simulated and measured absorption curves of OS-HMM absorber for (b) *x* polarization and (c) *y* polarization. (Reprinted with permission from [66].)

and 40.4 GHz. The absorption peaks were shifted to higher frequencies such as 9.8, 30.5, and 53 GHz when the thickness was reduced from 9 to 7 mm. The spiral FSS with 100 Ω resistance and 2 mm thickness showed absorption in the 18.5–52.4 GHz frequency range. Due to the grating lobes, several smaller peaks of reflection losses were observed for frequencies larger than 50 GHz. The multi-layer FSS combines all three FSSs, to obtain better absorptivity.

Conventional millimeter-wave absorbers are thick and bulky where the performance is controlled by permeability and permittivity. While, in the case of MMAs, any variation in geometry could lead to improved performance. In general, the bandwidths of MMAs are typically narrowband, since it depends on the resonance bandwidth of the resonant structure [53].

Sun *et al.* [30] proposed a broadband absorber using the concept of destructive interference. An MM with multi-layered split-ring resonators was used to obtain the desirable refractive index spectrum, which could induce anti-reflection in large bandwidth. The reflection from the two layers caused destructive interference, thus forming absorption. The resonances in ε and μ of the MM can be controlled to cause absorption of both electric and magnetic fields, which requires a resonator of a certain size and with low loss substrates. The successive anti-reflection causes large bandwidth absorption. However, despite using the SRR (split ring resonator), the resonance is not lossy enough to be called a perfect absorber but provides an optimum refractive index for causing destructive interference.

Multilayer resistive metasurface has also been used to develop broad absorption bandwidth and to achieve perfect impedance matching at resonant frequencies. Lumped elements or resistive films can also be used to obtain such broadband absorption [7, 28, 59, 60–65]. Yin *et al.* [66] combined two dissimilar tapered hyperbolic metamaterial (HMM) waveguide arrays into a unit cell as shown in Fig. 4. Each of these waveguides has wide and dissimilar absorption bands. HMMs consist of metal/dielectric multilayers, possessing a large number of applications [67–72]. After integrating these waveguide arrays, the broadband was achieved for the 2.3–40 GHz band, by varying the geometrical parameters and combining the absorption bands of the individual HMMs. This method is much preferred to discard the lower absorption bands that could appear in between the large bandwidth of the absorber.

A similar study was conducted in 2014 by Li *et al.* [73] where they combined two layers of hybrid absorbers and obtained >90% absorptivity for the 4–40 GHz range. A triple layer topology of MMAs was proposed in [74], comprising an array of resonators prepared from aluminum, deposited on the Kapton film substrate. This metal–dielectric–metal arrangement can be comprehended as a Fabry–Perot resonant cavity, where it helps in absorbing light between multilayered structures. The highly compact and flexible substrate helps in the integration of sensors on-chip.

Long and Zhiyong [32] proposed an ultra-wideband absorber that consisted of three metasurface layers, having three resonant modes. The thickness of the absorber was designed to be 3.8 mm. The absorptivity measured was found to be more than 80% from 7 to 37.4 GHz. Here, the dielectric substrate was F4B-2. The applicability can be checked using different substrate candidates and comparing the absorption efficiencies with each other.

The three metasurface layers can be varied with different thicknesses and resistivity also. Improving the absorption performance of the Salisbury screen was achieved in [75]. Here, the metasurface was used as the ground plane, rather than in the dielectric or the top layer of the absorber. The metasurface is capable of generating random phase responses and could control dispersion properties. This gives more degrees of freedom, helpful in broadening the bandwidth and good absorption performance of the conventional Salisbury screen. The absorption performance was studied for 6–30 GHz, with 133% fractional bandwidth, which was 85% better than a Salisbury screen with only 83% fractional bandwidth.

Some electronic applications require large light transmittance as well as absorbance. The optically transparent microwave system is an ongoing research area [36]. In the past, an optically transparent MA for low frequency has been prepared. A millimeter-wave absorber has a different requirement for the structures.

Early in 1999, Takizwa *et al.* proposed a transparent absorber consisting of resistive sheets, ITO, and polyethylene terephthalate (PET) with polycarbonate (PC) as the spacer. They adjusted the sheet resistance of the top and bottom ITO layers to obtain absorption at 60 GHz [37]. Thereafter, Soh *et al.* [76] proposed the transparent absorber for two frequencies, 60 and 76 GHz bands. The absorber comprised of a dielectric spacer and three transparent resistive films prepared from PET and ITO, whereas the spacer was prepared from PC.

https://doi.org/10.1017/S1759078722000162 Published online by Cambridge University Press

Lai *et al.* [36] proposed an optically transparent ultra-broadband MA using ITO glass. ITO was used as the transparent conducting medium on the top and bottom of the glass material. The sputtering process allowed ITO to be deposited onto the glass substrate of 1.1 mm thickness. This was followed by wet etching to obtain the entire structure. The absorption ratio was verified by simulation and after fabrication and was obtained as >0.8 for 15.6–39.1 GHz.

A similar study [34] used ITO and PET as the material, with ITO on the top and bottom planes. An absorption of >0.8 was observed from 19.9 to 51.8 GHz. The thickness of the ITO film was 185 nm in both experiments [34–36]. The analysis for the above was conducted for zero polarization angle of the incident EM wave. However, on changing the angle, it was observed that the absorption curve dropped for TM polarization faster than that of TE polarization. For $\theta \leq 30°$, the change in absorption spectrum was found to be negligible in both cases. Zhang *et al.* [35] proposed an optically transparent absorber with a ring shape as the basic element, consisting of a sandwich structure prepared from ITO and polyvinylchloride along with PET. The observed absorptivity was from 26.5 to 40 GHz for angles between 0 and 60° for both the TE and TM modes.

A single-band ITO MM was designed by Yin *et al.* [33] at 120.8 GHz with an absorptivity of more than 90%. This design being a single band, showed an interesting phenomenon, where, on changing the surface resistance of the ITO layers, one could observe characteristics of dual band also. This phenomenon could be used for applications requiring dual-band or more absorption techniques. Lu *et al.* [77] proposed an absorber based on tractable conductive plastic that was fabricated using three-dimensional (3D) printing, for 16.3–54.3 GHz frequency range with 108% fractional bandwidth.

Wu *et al.* [78] designed an optically transparent FSS-based absorber using a metal mesh structure and was fabricated using electrohydrodynamics printing technology. This method of printing is highly used in the area of millimeter-wave technology and is an economical technique with the capability of printing on pliant and flexible substrates. Due to the geometrical symmetry of the structure, polarization angle has no net effect on absorption. This property is useful for several applications.

3D absorbers

Another approach to develop absorbers with low weight and low cost are 3D MMs. These absorbers show very high absorptivity from microwave to visible spectra. Tang *et al.* [48] proposed a 3D MMA prepared from nine resistive films of different sizes, mounted vertically on a metal plate. It showed an absorptivity of 90% for both TE and TM waves, in the 20–55 GHz frequency range. However, the proposed absorber was polarization-sensitive and can be used for polarization detectors, sensors, imaging, etc.

A 3D MMA consisting of resistive films and copper was designed, for normal incidence polarization, covering the 58.6–91.4 GHz frequency band. However, the design was complex and needed very careful precision while fabricating [79]. Another multilayered, 3D structure was proposed by Ling *et al.* [49] which consisted of six resistive films placed on the ground plane. It consisted of mainly two layers, having six resistive films of different sizes, having square-shaped open rings. An ultra-broadband absorption was achieved from 38 to 142 GHz, with a wide incident and polarization angle.

Vahidi *et al.* [80] designed a novel 3D absorber, having six-fold symmetry, consisting of a periodic honeycomb-like structure. The proposed design obtained more than 90% absorptivity in the 50–460 GHz frequency range. These designs were highly flexible, which could have applications extending to terahertz, infrared (IR), and visible ranges. They can be useful in imaging, sensing, and camouflaging technology. Petroff *et al.* [81] designed an absorber using an additive manufacturing process with a fused filament fabrication. The design was achieved using a Hilbert curve which is also known as the space-filling curve as shown in Fig. 5.

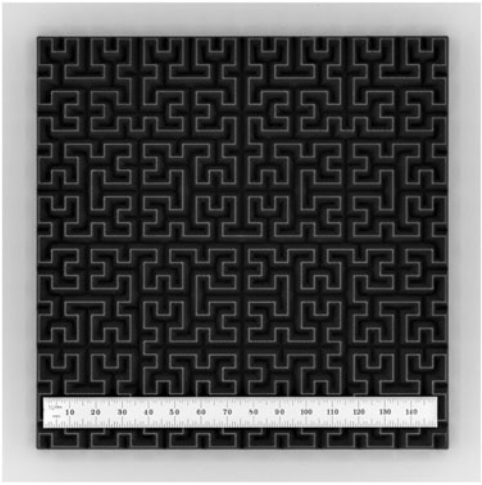


Fig. 5. Prototype carbon-loaded HIPS Hilbert curve absorber. The footprint of the absorber is 160 mm square. (Reprinted with permission from [81].)

Another graded-index millimeter-wave absorber using a 3D printed mold was prepared by Adachi *et al.* [82]. This mold had a pyramidal shape and absorbing material inside the mold. The unmolding step is not necessary if the 3D-printed mold is transparent within the millimeter-wave frequency range.

However, there is a limited option for the absorptive material to be selected in this case. Also, the advantage of this method was the optimization of thermal conductivity.

The advantage of using a 3D structure for absorption is its smaller unit cell size than the operating wavelength, as compared to the conventional 2D structures. This helps position it at the curved surface. It offers the ability to individually control the defined thickness of the designed unit cells. Therefore, it can counter the effects of curvature more flexibly [83].

However, 3D structures pose difficulty in the fabrication process, though, this can be compensated by its exceptional performance.

Table 3 shows the comparative study of the discussed millimeter-wave absorbers.

Based on polymer composites

Out of all the materials used in designing absorbers, the most popular has been the use of polymers, i.e. carbon-based materials. EM radiation can also interact with polymers through the most prominent absorption phenomenon. For frequencies <1 THz, EM waves are absorbed by those polymers which consist of polar groups, thus causing orientation polarization, which in turn generates heat. The absorption of IR radiation causes atomic vibrations, but there is no breaking of bonds, i.e. they do not undergo chemical reactions. However, visible and ultraviolet light interacts with inner shell electrons in the atom, undergoing

https://doi.org/10.1017/S1759078722000162 Published online by Cambridge University Press

Table 3. Comparative list of recently reported broadband millimeter-wave absorbers arranged in ascending order of year of publication

Year	Frequency range (GHz)	Absorptivity (%)	Thickness (mm)	Polarization	Incidence angle	Ref.
2011	77–110	>90	0.126	Sensitive	Normal incidence	[52]
2013	90.4–100	>95	6.57	Insensitive	0–45°	[38]
2015	2.3–40	>80	11.5	Insensitive	0–60°	[66]
2015	6.57–28.1	>60	4	Sensitive	Normal incidence	[84]
2016	26.9–32.9	>90	2.25	Insensitive	0–30°	[85]
2016	38–142	>90	1	Insensitive	0–60°	[49]
2016	58.6–91.4	>90	0.5	Insensitive	10–70°	[79]
2016	90–100	>60	0.12	Insensitive	Normal incidence	[54]
2016	20–55	>90	0.1	Insensitive	0–60°	[48]
2017	17–42	>90	1.5	Insensitive	0–50°	[86]
2017	6–30	>85	4.4	Insensitive	Normal incidence	[75]
2017	20.59–43.73	>80	0.92	Insensitive	0–90°	[87]
2017	7–37.4	>90	3.8	Insensitive	0–90°	[32]
2017	15.6–39.6	>80	1.1	Insensitive	0–30°	[36]
2018	65.38–67.86	>90	0.5	Insensitive	0–120°	[88]
2018	90–140	>88	0.05	Insensitive	0–60°	[89]
2018	50–460	>90	1	Insensitive	0–70°	[80]
2018	14.2–32.3	>60	2.6	Sensitive	0–45°	[90]
2018	100–140	94.1	1.1	Insensitive	0–60°	[33]
2018	16.3–54.3	>90	2.7	Insensitive	0–45°	[77]
2018	19.9–51.8	>80	1.1	Insensitive	0–60°	[34]
2019	98–353	>90	0.1	Insensitive	0–45°	[91]
2019	6.9–29.9	>80	3.89	Insensitive	0–45°	[92]
2019	26.5–40	>80	1.65	Insensitive	0–45°	[35]
2020	73.5–110	>90	0.525	Insensitive	0–45°	[78]

chemical reactions. Even for frequencies higher than 10^{15} Hz, light interacts with shell electrons, causing chemical changes. The energy of a photon is thrice the magnitude lower than the binding energy in an atom. If sub-THz radiation is absorbed, there is a generation of heat, converting photonic energy to translational energy. This generation of heat is known as dielectric loss heating. This is because polar materials with permanent dipole moments are capable of absorbing sub-THz radiation. For absorption, EM radiation is an important measure to help in the synthesis processes of polymers via the polymerization of small molecules.

Some of the applications of the interaction of EM radiation with polymers are microwave heating useful for the vulcanization of rubber, recycling of polymeric waste, and industrial processing of polymeric materials [93]. Commonly used polymers for the development of millimeter-wave absorbers are graphene, CNTs, epoxy resins, and polyaniline (PANI). We will discuss these below.

Single-layered absorbers

Using epoxy resins. Epoxy resins are a very useful thermosetting polymer that are used as matrixes, with exceptionally good mechanical strength, chemical stability, heat stability, low contractibility, strong adherence, excellent electrical properties, dielectric constant, less shrinkage, chemical resistance, mechanical resistance, and a stable strength to weight [94]. Epoxy resins are used for coating and sheathing the electrical circuit components where they protect the electrical devices from adverse effects of atmospheric changes, moisture, leaking current, mechanical shock, and vibrations. For the use of epoxy resins in electronics, the primary importance is of their dielectric constant which is 3–6 at normal temperature and low frequencies. Compared with other polymeric composites, epoxy is cheaper, easy to produce, and the amount of yield produced is in bulk, which can be used in several slots.

An absorber using epoxy-modified urethane rubber mixed with carbon particles was designed by Soh *et al.* in the range of 54–60 GHz [95]. In 2000, the authors designed an absorber using the same material, i.e. epoxy-modified urethane rubber mixed with carbon particles, and the absorption characteristics were calculated in the 50–110 GHz range, where the peaks were observed at 60 and 110 GHz [96]. Similarly, the authors also proposed absorption peaks at 76 or 94 GHz bands using the same materials [97]. This was the earliest research study in the millimeter-wave range. Also, in 2003, the authors studied the absorption behavior of titanium dioxide (TiO_2) and epoxy resin containing carbon particles. The absorption peak shows variation in the range of 50–110 GHz.

https://doi.org/10.1017/S1759078722000162 Published online by Cambridge University Press

Here, epoxy resin is resistant to weather variations. The high permittivity of TiO_2 and carbon particles proved to help design the absorber by satisfying the reflectionless conditions for absorption. In applications related to electronic packaging, it is challenging to achieve the requirements of EM wave absorption, namely (a) large reflection loss, (b) thin coating of the absorber, which would lessen the weight and thus, the cost also reduces (c) good compatibility with materials used for electronic packaging, so that it can be easily realized in the industry using epoxy resin or polyimide.

Xiao *et al.* [98] reported a novel epoxy-based absorber, where BNFO ($BaNb_{0.6}Fe_{11.4}O_{19}$) was doped with epoxy and for electronic packaging applications. BNFO is used as a filler that can generate large dielectric and magnetic losses at once. Epoxy resin is used as a matrix since it is a typical material used for electronic packaging applications. As the BNFO content increased from 40 to 75 wt%, the improvement in matching conditions was observed with good absorption. The 60 and 75 wt% content of BNFO gave good absorption, with 13.5 GHz bandwidth in the 26.5–40 GHz range. The real and imaginary parts of permittivity increased as the content of BNFO increased. The real part of permittivity of epoxy is around 2.3, but it increased from 3.33 to 7.48, as the content of BNFO increased from 20 to 75 wt%. The imaginary part of permittivity of epoxy is 0.09, which increased from 0.32 to more than 2.25, as the content of BNFO increased from 20 to 75 wt%. A similar trend was observed for permeability also. The matching thickness showed a decrease from 1.09 to 0.97 mm as the content of BNFO increased from 40 to 75 wt%.

Due to the high weight content, the overall structure was bulky. Also, when the content of BNFO was above 40%, they observed a peak in the imaginary part of permittivity, which, though has been reported earlier, but is still under controversy and needs thorough investigation.

The epoxy resin composites filled with two types of commercially available graphitic particles, exfoliated graphite and thick graphite in 0.25–2 wt% was used in [99]. It was shown that epoxy composites of 1–2 wt% provided good EMI shielding both at microwave as well as THz frequencies. Though it was light weight, its absorption efficiency was quite poor.

Carbon nanocoil (CNC)-based composites were prepared by dispersion in epoxy resin through ultra-sonication with low concentration (0.1–1 wt%) by Suda *et al.* [100]. These novel CNC-based composites showed good absorption property in the W band (75–110 GHz). The solvent formed large agglomerations, causing irregularities on the absorber surface, making it difficult to maintain the thickness of the absorber constant. The effects of the chiral constant were not considered while deriving the permittivity, which can make it difficult to study the characteristic impedance of the absorber.

Epoxy resin was mixed with CNT and barium titanate (BT) fillers in [41] by Lozitsky *et al.*, for 1–5 wt% of CNTs and 34 wt% of BT. Ferroelectric ceramics such as BT is commonly used to increase the dielectric parameters of polymeric composites. The absorber properties were studied from 1 to 67 GHz. The highest absorption was obtained for 10–65 GHz for 2 and 3 wt% CNTs.

The BaM + $BaTiO_3$ with PANI composites was added as a filler into epoxy resin and polyethylene and synthesized via *in situ* polymerization process and was tested in the frequency range 2–40 GHz, where absorption bands were obtained at 9.6, 31, and 38.2. The magneto-electric effects caused the generation of electric and magnetic losses, and by the changes in the microwave field at the interface between the blend and polymer. The good absorption efficiency with the low cost and easier preparation mechanisms was observed in this case [101].

Using graphene. Currently, graphene is widely used in scientific research due to its properties such as high electrical and thermal conductivity and mechanical strength. The surface area of graphene is high, which makes them a good charge carrier. Graphene is a 2D structure of carbon connected in a covalent bond with the free-electron cloud of carbon which is perpendicular to the hexagonal plane. Due to this, there is a π–π interaction between the graphene sheets. But there may be the generation of several defects and dangling bonds, during the synthesis process. This leads to a lower intrinsic value of conductivity. These defects and dangling bonds result in the formation of different permanent polarization, which contributes to the absorption of EM waves. Though the defects and functional groups present in the graphene, at times limits the electrical conductivity, it has been still used for EM absorption purposes [102]. When graphene is mixed with polymers, the obtained composite has more advantageous properties than when it is used individually. The graphene composite forms a bond with each other to form a highly conductive system. Because of this, conductive losses can occur in the network. The microwave absorption process in graphene is a result of combined effects of polarization, conductive losses, interfacial, and multiple scattering. Graphene is tunable and has a surface impedance that is independent of frequency. This property is useful for impedance matching and thus, good absorption.

Zhu and Li [103] proposed a tunable wideband absorber that was designed using graphene patterns as an FSS placed on a dielectric substrate. By varying the conductivity of graphene, the absorptivity also changed. Setting the chemical potential to 0.3 eV, it was found that absorptance was 90% in 25.4–93.9 GHz. On expanding the unit cell, the working frequency was also observed to scale down.

Zhang *et al.* [104] made use of a 3D free-standing graphene foam composite. That study reported enhanced absorption performance with a bandwidth of 50.5 GHz in the range, 2–18, 26.5–40, and 75–110 GHz. On tuning via physical compression, it has shown to change its absorption bandwidth, i.e. on 90% compression strain, it gives a bandwidth of 60.5 GHz, covering 93.8% of the entire bandwidth and about 70% wider than that of previously reported literature. The 3D conductive network of graphene foam can be used for applications of light and tunable high-performance absorption, such as electronic surveillance and stealth technology units with high payload.

Two-resistive patterned single-layered graphene was mounted on the dielectric substrate. It achieved absorptivity of 90% in 9.2–200 GHz [105].

Ma *et al.* [106] showed the tunable and broadband absorption performance of 3D porous MXene/graphene oxide (GO) foam which covered the frequency range on the higher end of millimeter-wave, 200 GHz to 2 THz. A large number of nanometer porous structures cause multi-reflections of the EM waves. Introduction of MXene was shown to help in improving absorption performance. However, it was observed that when the ratio of masses of MXene and GO nanosheets are more than 1:5, absorptance does not increase.

Using CNTs. One of the important allotropes of carbon known as CNT or carbon nanotubes contains sp^2 carbon, which has shown good EM wave absorption properties in the past. They have strong mechanical properties, with a tensile strength of 50–500 GPa and an elastic modulus value of 1 TPa. CNTs can be prepared to realize strong semiconducting properties and

https://doi.org/10.1017/S1759078722000162 Published online by Cambridge University Press

high charge mobility and current-carrying ability [44]. CNTs are non-magnetic, thus, the absorption process originates from polarization, ohmic losses, or multiple scattering. Different types of CNTs, namely single-walled CNTs (SWCNTs) and multi-walled CNTs (MWCNTs) have been used as MAs in the past [46].

Compared to SWCNTs, MWCNTs have larger defects due to their complex structure and large permittivity. Dielectric relaxation phenomena lead to absorption in this case. As the content of CNT increases, its percolation threshold affects its effective dielectric permittivity largely and hence the absorption characteristics.

MWCNTs can be added with non-woven fabric to achieve more than 95% absorption as shown by Sano and Akiba [107].

A theoretical model was developed to study the characterization of nanomaterial by Nefedova *et al.* [108]. To use this method numerically, it is important to study the material in a detailed manner. A CNT was placed randomly on a dielectric rod waveguide. It was measured from 75 to 110 GHz. Composite CNT films were studied in [109] due to their EMI-shielding effectiveness. The macro-films of CNT strongly adhered to the surface of the common cloth. This was obtained in the 40–60 GHz frequency range.

Using the properties of the waveguide of metallic honeycomb structure filled with PC foam and thermoplastic polyurethane reinforced with CNTs [43], absorption was obtained in the 5–40 GHz frequency range. For low weight content of CNTs dispersed inside the matrix, there is a good amount of attenuation. This is due to the aspect ratio which helps in the formation of a conductive network. However, it was difficult to achieve a good absorption index below 5 GHz, by keeping acceptable material thickness and cell size.

A graphene-vertically aligned CNT (G-VACNT) hybrid was proposed and designed for frequencies covering above 200 GHz to 3 THz [42]. The absorber consisted of Cu/PDMS/graphene/VACNT layers placed upon the PET substrate. The VACNT is used for its low reflection with enhanced absorptivity at high frequencies. This structural arrangement was used for absorption at lower THz frequencies, from 200 GHz to 3 THz.

This can be highly flexible and can have wafer-scale fabrication. It can be used in applications such as bolometric imaging and energy harvesting.

Using polyaniline. PANI and its composites have been studied extensively in the past due to their microwave absorbing properties. They are inexpensive, easier to prepare, stable in both doped and undoped forms, have excellent chemical and physical properties, and good conductivity at microwave frequencies [110]. The microwave absorbing properties of PANI originate from the fact that it is non-magnetic. The composites are prepared via polymerization techniques and mixing. Blending PANI with certain insulating polymers can improve the physical and chemical properties of PANI without any alteration in its structure. Among all the conducting polymers, PANI has shown a simpler synthesis process and environmental stability. PANI has been integrated with magnetic materials and conducting polymers [111, 112].

The synthesis of the composite of chiral PANI and Barium hexaferrite (BF) was achieved in [113] for the first time. BF is known to have a good magnetic property, also used in the development of MAs. But, when it is used alone, there is a large difference between the values of effective permittivity and permeability. This large difference creates impedance mismatch, thus reducing the effective absorptivity [113].

Here, the composite developed was light weight, environmentally stable, and corrosion-resistant and the absorption above 90% was obtained for K_a-band. The good absorption was attributed to the balance between permittivity and permeability, due to the presence of both magnetic as well as dielectric elements.

Multi-layered absorbers

Using epoxy resin. A graded-index absorber was designed by Xu *et al.* [114]. The anti-reflection mechanism was achieved by tuning the dopant concentration of the polymer composites. To achieve a perfect reflection difference, the refractive index value of the matrix, epoxy resin was tuned by hollow PC microspheres and TiO_2 nanoparticles. With a highly doped Si substrate and six layers of the structure, 98% absorption was achieved from 100 GHz to 20 THz.

Epoxy-based composites using graphene for 200–320 GHz were reported [115], where the transmission was found to be very less, even at small concentrations of fillers. The higher doping concentration of graphene improves the heat conductivity properties, but on the other hand, also increases reflections. So, it is important to scale the graphene content as much as to improve the heat conductivity without any increase in reflection. Here, the graphene content was low, which ensured the low cost of the absorber. The absorptivity of more than 95% is achieved when the content of graphene was 1 wt%.

Using graphene. Batrakov *et al.* [116] used the inclined geometry that increased the conductivity of graphene films, and compared the two possible dielectrics, quartz and epoxy as the substrates for the maximum absorptivity. The absorptivity of 80% was obtained at 30 GHz and 65% at 1 THz.

Liu *et al.* [117] designed a thin absorber by placing a Jerusalem-shaped patch prepared from graphene in between the dielectric layers. The unit cell consisted of four layers, a graphene-resistive pattern, and two dielectrics, having the same thickness and permittivity, and a ground plane. It was shown that with an increase in the permittivity of dielectric slabs, the bandwidth decreases but there is hardly any change in the fractional bandwidth. An increase in the thickness of the substrate decreases the bandwidth and fractional bandwidth. It was shown that when the permittivity ($\varepsilon_r = 2$), the wide absorption was obtained from 10.2 to 43.5 GHz with the fractional bandwidth of 124%.

The design was bulky and that as the chemical potential is increased, bandwidth increases but at the cost of absorptivity. A composite of magnetic iron particles and expanded graphite was prepared by Hung *et al.* [118]. It is to be reminded that graphite is composed of several layers of graphene. In the above case, the composite gave good attenuation properties in 32–38 GHz.

Chen *et al.* [119] designed an excellent millimeter-wave absorber for 5G applications, where elastic absorbing composites were fabricated using reduced graphene oxide (RGO) with different reducing times along with nitrile butadiene rubber (NBR). The dihedral angles formed by the stacks of RGO sheets cause multiple reflections thus, laying the foundation of a good absorption mechanism. The RGO/NBR composites with a reduction time of 3, 5, 7 h were prepared, out of which 3 h-RGO/NBR exhibited the best absorption performance at 35.4 GHz. The study was conducted for the K_a-band.

Wu *et al.* [120] reported the fabrication of transparent absorbers, consisting of multilayered graphene sheets, put on top of a quartz substrate with a grounded metal plate. The graphenes were prepared using the chemical vapor deposition method.

https://doi.org/10.1017/S1759078722000162 Published online by Cambridge University Press

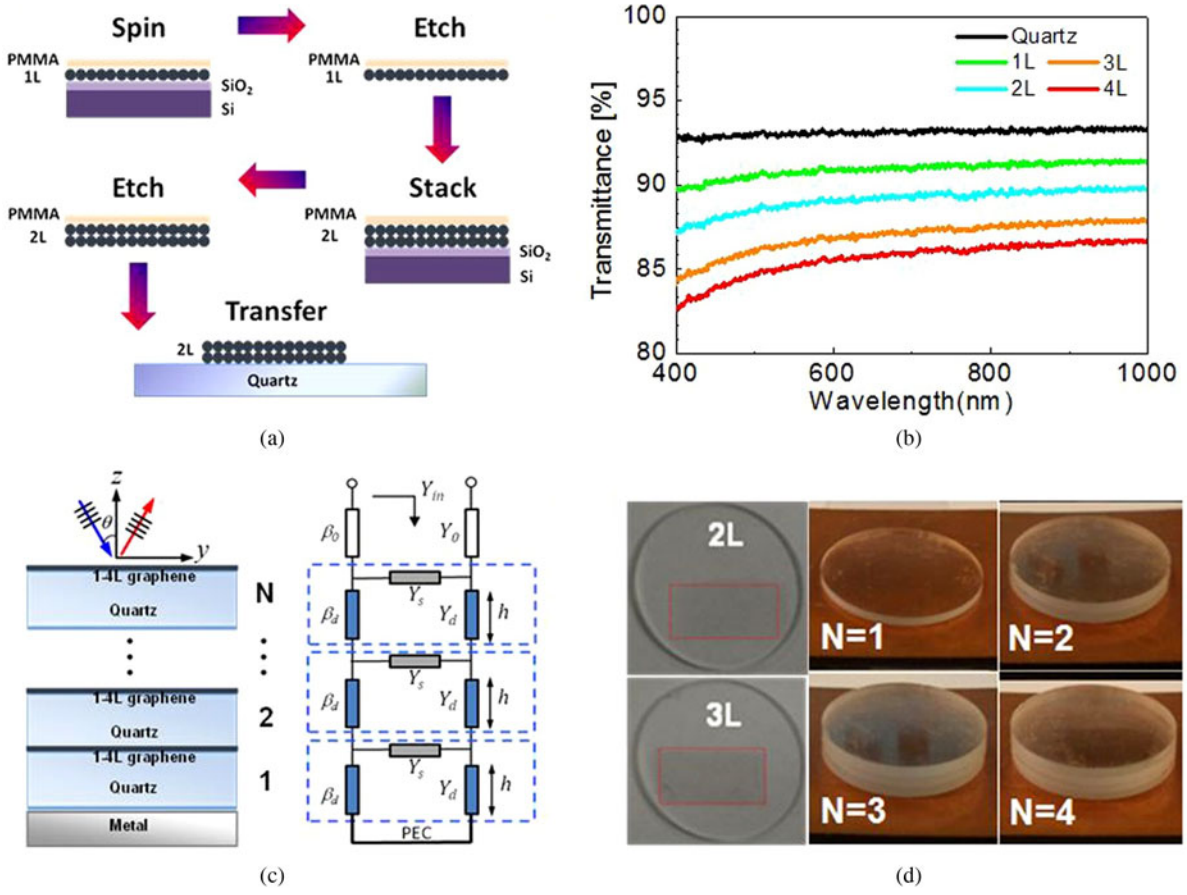


Fig. 6. (a) Representation of an etch and transfer preparation process for a two-layered device, (b) UV-Vis spectra for 1–4-layered graphene samples, (c) schematic representation of the *N* layered absorber with its equivalent circuital model, and (d) optical images of 2 and 3 layered absorbers and *N* = 1 to 4 graphene-quartz stacked samples. (Reproduced with permission from [120].)

The multilayered graphene sheets were produced by the repeated procedure of etching and transfer as shown in Fig. 6. This method was used to minimize the PMMA residues and thereby producing high-quality and optically transparent graphene films. It is important to note that, each graphene–quartz layer forms a Fabry–Perot resonator. When the graphene–quartz samples are layered together, they form a mutual coupling, which gives rise to multiple absorption peaks, hence creating broadband. On verifying it experimentally, it was found that for five layered structures, 90% absorption efficiency was obtained from 125 to 165 GHz, with a fractional bandwidth of 28%. However, a thin-layered graphene absorber could be developed, with relatively less cost. Also, different structural absorbers could be realized to study the EM properties. Batrakov *et al.* [28] demonstrated in his work, that sandwiched PMMA thin films between the graphene layers have very good absorption efficiency. This was done for the frequency range of 26.5–40 GHz. At around 30 GHz, the absorption was highest when the number of graphene layers was six. Increasing the number of layers reduced the absorption efficiency. Using a small thickness layered structure with high absorption would be applicable for nanodevices. PMMA/graphene multilayers have proven to be flexible shielding materials. The process of preparation is shown in Fig. 7.

This was further improved by Mencarelli *et al.* [121] who proposed multi-layer PMMA/graphene for high-EM absorption in the millimeter-wave frequency range. The optimization was done by properly patterning the multi-layered structure. The graphene layers were perforated with holes of a controlled radius.

The average conductance of the graphene layers was varied and absorption efficiency was measured. For the conductance of 0.8 mS, absorption of more than 75% was observed with small ripples as compared to the conductance of 0.3 mS, with 100% absorption and a large number of ripples. The designed absorber has been reported for use in innovative surface and coatings, not only absorption.

Using CNTs. Danlee *et al.* [122] used PC and CNT to design an MMA. A good absorber needs to have antagonistic properties, meaning, it must have a certain conductivity level along with a low dielectric constant. Since these properties are not found naturally, these can be designed artificially, which was done by Danlee *et al.* They designed a thin and flexible absorbing solution, which could be used to isolate any electronic, medical devices from EMI. They used PC to homogeneously disperse CNT. The shape of CNT helps in lowering the percolation threshold to a smaller percentage of weight. Absorption of above 80% was observed for 10–40 GHz. This method showed an arrangement of successive dielectric and conducting layers, to create a conducting gradient. This method can be used for higher frequencies, with modifications in thickness and conductivity.

This study was extended and applied by the authors in [44] where the applicability of the gradient-multilayer method was extended in that study by patterning the conductive layers as

https://doi.org/10.1017/S1759078722000162 Published online by Cambridge University Press

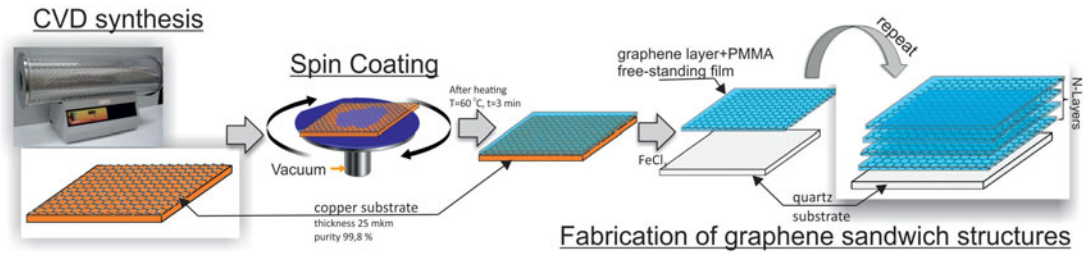


Fig. 7. Representation of graphene sandwich fabrication, with several repeating steps and final PMMA/graphene structure, is formed. (Reproduced with permission from [28].)

strip lines, which thereafter induces strong anisotropy leading to a good absorption property. The designed absorber was polarization-dependent, using CNT deposited on PC sheets. However, the main requirement of this absorber was that the ratio between gaps between conductive strip lines to its width must be 5.

Biswas *et al.* [123] designed a millimeter-wave absorber by choosing a polymeric blend of immiscible solution of PC and

Table 4. Comparative list of recently reported polymeric millimeter-wave absorbers arranged in the ascending order of year of publication

Year	Polymer	Layer	Absorptivity (%)	Frequency (GHz)	Thickness (mm)	Ref.
2011	Epoxy	–	>90	2–40	2	[101]
2012	CNTs	Eight	>90	10–40	2.7	[122]
2012	CNTs	Single	80	5–40	7	[43]
2014	Graphene	Five	>90	125–165	1.3	[120]
2014	Graphene	Six	54	26.5–40	0.042	[28]
2014	MWCNTs	Single	95	50–66	0.5	[107]
2014	PANI	Single	>90	26.5–40	0.9	[111]
2014	PANI	Double	>90	26.5–40	1	[129]
2015	Epoxy	Single	>60	26–37 100 GHz–3 THz	1	[99]
2015	Graphene	Single	>90	25.4–93.9	1.2	[103]
2015	Graphene foam	Single	>90	2–18, 26.5–40, 75–110	1	[104]
2015	CNTs	Single	>80	40–60	0.04	[109]
2015	CNTs	Single	>90	75–110	6.00×10^{-5}	[108]
2015	Tannin carbon foam	Single	>80	20 Hz–35 GHz	2	[136]
2016	Epoxy	Six	>90	100 GHz–I THz	3.2	[114]
2016	Graphene	Five	>80	30 GHz–l THz	0.5	[116]
2016	Graphene	Single	>95	39.2–200	0.74	[105]
2016	Graphene	Multi-layered	>90	30–300	1	[121]
2016	CNTs	Four	>90	10–60	1.15	[44]
2016	Silicon resin	–	>90	55–67	2	[113]
2016	Silicone rubber	Double/multi-layered	>90	32–38	1.5	[118]
2017	Phytoporous	Single	90	73–90	2	[134]
2018	CNC	Single	>90	75–110	2	[100]
2018	Graphene	Four	>90	10.2–43.5	4	[117]
2018	CNTs	Two to five	>90	75–110	0.001	[45]
2019	Epoxy	Single	>90	26.5–40	0.98	[98]
2019	RGO	Few layer graphene	>90	26.5–40	2–2.5	[119]
2019	GO foam	Single	>90	200 GHz–2 THz	4	[106]
2020	Graphene	Few layer graphene	>90	220–325	1	[115]
2020	VACNTs	Single	>98	200 GHz–3 THz	2.6	[42]

https://doi.org/10.1017/S1759078722000162 Published online by Cambridge University Press

polyvinylidene difluoride. To achieve absorption of EM wave radiation, the two most important key factors, high conductivity and large loss characteristics were achieved by incorporating MWCNTs. The addition of magnetic Fe_3O_4 clusters exhibited efficient heat dissipation, high absorptivity due to the presence of electric and magnetic dipoles, making it suitable for developing millimeter-wave absorbers.

Using a metallic waveguide structure for embedding CNT-based absorbers [45] using various preparation methods is also important in determining its usefulness. Here, the experiment was held for 75–110 GHz, where the absorber which was a CNT-based material was highly porous aerogel, prepared by freeze-drying technique.

The advantage of this method is that the porous structure formed has random orientations and offers low surface reflections, hence enabling effective absorption. This method of preparation can be extended beyond THz applications.

Combining CNTs with cement was achieved [124] where the cement matrix of the absorber has electrically conductive paths, which are isolated from each other and a CNT forms a resistor/capacitor structure with excellent dielectric behavior.

Using polyaniline. The new composite materials formed have improved applications and properties in microwave absorption. M-type BF (barium ferrite) is a potential material for microwave absorption since it has large magneto-crystalline anisotropy, large magnetization, and Curie temperature [125]. The electric and magnetic properties must be modified to obtain improved properties. Ting and Wu [126] synthesized PANI/Ba ferrite composite via *in situ* polymerization method. Good absorption properties were exhibited in the frequency range of 2–40 GHz. This composite was synthesized via *in situ* polymerization and showed excellent millimeter-wave absorption properties in the range of 2–40 GHz. Magnetite (Fe_3O_4) has not only the strongest magnetic properties, but it also has excellent EM-absorbing properties [127].

Belaabed *et al.* [128] showed that addition of magnetite dopants improves the EM-absorbing properties of the PANI composite. Xu *et al.* [129] designed a double-layered millimeter-wave absorber with PANI and PANI/Fe_3O_4, where PANI was a matching layer and the latter was an absorbing layer, the absorption efficiency was highest at 33.72 GHz. The total bandwidth was 11.28 GHz, with a frequency from 27.24 to 38.52 GHz. Bamboo charcoal coated with PANI was prepared at different weight ratios and introduced into epoxy resin. At higher weight content, the electrical conductivity of BC/PANI increased, implying that PANI improves electrical conductivity. These composites exhibited good absorption performance in the range of 2–40 GHz. The difference in the absorption peaks implies the dielectric and magnetic loss which was generated by the magnetic dipoles and by the change in boundary condition of the microwave field at the interface of the prepared composite and the polymer matrix [130]. Few rare-earth elements have been added to PANI to observe a good absorption efficiency [131].

Yu *et al.* [132] developed cerium oxide doped in PANI/Al-alloy foams with doping of cerium oxide in 1, 2, and 5%. This showed excellent absorption in 12–18 and 26.5–40 GHz. Yu [133] developed another rare-earth doped in PANI/Al-alloy foams as a composite material to develop the absorber in 12–18 and 26.5–40 GHz. The absorption increased by increasing the frequency. The rare-earth doped in PANI did not change the shape of PANI, as was observed in the scanning electron microscopy images, indicating the uniform dispersion of the particles. The absorption of pure PANI, 2% doping of rare earth, and 5% doping, increased with the increase of frequency.

Conclusion

This review provides an insight into the progress in the development of millimeter-wave absorbers and challenges faced by microwave/RF designers. The development of low-cost, thin, and polarization-independent absorbers with maximum efficiency has been shown. It primarily focuses on the classification of geometrical as well as material-based designing of the broadband millimeter-wave absorbers with their shortcomings as well as their applications. Polymeric composites have been shown to find application in the development of flexible and tunable absorbers. Various polymer composites such as CNTs, graphene, epoxy resins, and carbon gels have been used to develop absorbers in the millimeter-wave frequency range. Compared with conventional EM absorber polymeric materials, the highly demanded 3D graphene guarantees promising results in EM wave absorption. When graphene is combined with polymers, the formed composites add precedence not only in the EM-absorbing ability, but also they are low weight, flexibility, and low cost.

Agricultural residues which are not suitable for human consumption have also been used for developing millimeter-wave absorbers [134]. These residues preserve properties such as light weight, high heat retention, good absorptivity, and high permittivity, which are the primary requirements for developing high-quality absorbers. Absorbers using such residues have not been used much for the millimeter-wave frequency band. Some carbon-based magnetic composites have been used for EM absorption in the lower gigahertz range. Very few studies have been conducted for the millimeter-wave range, using carbon-based magnetic composites [135]. Absorbers using silicon resin [113] and tannin [136] have also shown good absorption efficiency. Table 4 shows the comparative study of the various polymeric millimeter-wave absorbers discussed in this paper.

For different frequency bands in the EM wave spectrum, there are various applications of millimeter-wave absorbers. These absorbers have found use in diverse areas of technology, though initially it was used for concealment and enhancing radar efficiency. These are widely used in the defense sector, where there is a need to develop radar-absorbing materials and improving the radar characteristics.

The radar-absorbing materials are widely used in stealth technologies and as EMI shielding for high reflection surfaces. The stealth technology is the most typical application of EM wave absorption. This method is useful for escaping the detection of aircraft by reducing the radar cross-section area. Other electrical applications include reducing the negative impacts of cavity resonance in the integrated microwave circuits, thermal sensors [137], healthcare [138], and frequency-related sensors [139]. Several of the electronic appliances use absorbers in their circuits for diversified uses such as amplifiers [140], filters [139], switches [84], and bolometers [3]. It is also used in high rising buildings, for prevention of EMI, for preventing leaking waves of the microwave oven, for protection of local area networks, and in anechoic chambers. These are also used for developing isolation in electronic devices and mobile communications [85–92, 141].

https://doi.org/10.1017/S1759078722000162 Published online by Cambridge University Press

References

1. **Munk BA** (2009) *Metamaterials: Critique and Alternatives*. Hoboken, NJ: John Wiley & Sons.
2. **Caloz C and Itoh T** (2005) *Electromagnetic Metamaterials: Transmission Line Theory and Microwave Applications*. New York: John Wiley & Sons.
3. **Landy NI, Sajuyigbe S, Mock JJ, Smith DR and Padilla WJ** (2008) Perfect metamaterial absorber. *Physical Review Letters* **100**, 207402.
4. **Watts CM, Liu X and Padilla WJ** (2012) Metamaterial electromagnetic wave absorbers. *Advanced Materials* **24**, OP98–OP120.
5. **Liu Q, Xu X, Xia W, Che R, Chen C, Cao Q and He J** (2015) Dependency of magnetic microwave absorption on surface architecture of $Co_{20}Ni_{80}$ hierarchical structures studied by electron holography. *Nanoscale* **7**, 1736–1743.
6. **Lv H, Ji G, Wang M, Shang C, Zhang H and Du Y** (2014) Hexagonal-cone like of $Fe_{50}Co_{50}$ with broad frequency microwave absorption: effect of ultrasonic irradiation time. *Journal of Alloys and Compounds* **615**, 1037–1042.
7. **Wang F, Wang X, Zhu J, Yang H, Kong X and Liu X** (2016) Lightweight $NiFe_2O_4$ with controllable 3D network structure and enhanced microwave absorbing properties. *Scientific Reports* **6**, 37892.
8. **Ji R, Cao C, Chen Z, Zhai H and Bai J** (2014) Solvothermal synthesis of $Co_xFe_{3-x}O_4$ spheres and their microwave absorption properties. *Journal of Materials Chemistry C* **2**, 5944–5953.
9. **Shah A, Wang Y, Huang H, Zhang L, Wang D, Zhou L, Duan Y, Dong X and Zhang Z** (2015) Microwave absorption and flexural properties of Fe nanoparticle/carbon fiber/epoxy resin composite plates. *Composite Structures* **131**, 1132–1141.
10. **Makarova TL, Geydt P, Zakharchuk I, Lahderanta E, Komlev AA, Zyrianova AA, Kanygin MA, Sedelnikova OV, Suslyaev VI, Bulusheva LG and Okotrub AV** (2016) Correlation between manufacturing processes and anisotropic magnetic and electromagnetic properties of carbon nanotube/polystyrene composites. *Composites Part B: Engineering* **91**, 505–512.
11. **Nam IW, Lee HK and Jang JH** (2011) Electromagnetic interference shielding/absorbing characteristics of CNT-embedded epoxy composites. *Composites Part A: Applied Science and Manufacturing* **42**, 1110–1118.
12. **Zhang H, Zhang J and Zhang H** (2007) Electromagnetic properties of silicon carbide foams and their composites with silicon dioxide as matrix in X-band. *Composites Part A: Applied Science and Manufacturing* **38**, 602–608.
13. **Tian C, Du Y, Xu P, Qiang R, Wang Y, Ding D, Xue J, Ma J, Zhao H and Han X** (2015) Constructing uniform core–shell PPy@PANI composites with tunable shell thickness toward enhancement in microwave absorption. *ACS Applied Materials & Interfaces* **7**, 20090–20099.
14. **Zou C, Yao Y, Wei N, Gong Y, Fu W, Wang M, Jiang L, Liao X, Yin G, Huang Z and Chen X** (2015) Electromagnetic wave absorption properties of mesoporous Fe_3O_4/C nanocomposites. *Composites Part B: Engineering* **77**, 209–214.
15. **Gnidakouong JRN, Kim M, Park HW, Park Y-B, Jeong HS, Jung YB, Ahn SK, Han K and Park J-M** (2013) Electromagnetic interference shielding of composites consisting of a polyester matrix and carbon nanotube-coated fiber reinforcement. *Composites Part A: Applied Science and Manufacturing* **50**, 73–80.
16. **Meng F, Wang H, Huang F, Guo Y, Wang Z, Hui D and Zhou Z** (2018) Graphene-based microwave absorbing composites: a review and prospective. *Composites Part B: Engineering* **137**, 260–277.
17. **Lu M-M, Cao W-Q, Shi H-L, Fang X-Y, Yang J, Hou Z-L, Jin H-B, Wang W-Z, Yuan J and Cao M-S** (2014) Multi-wall carbon nanotubes decorated with ZnO nanocrystals: mild solution-process synthesis and highly efficient microwave absorption properties at elevated temperature. *Journal of Materials Chemistry A* **2**, 10540–10547.
18. **Lu M, Wang X, Cao W, Yuan J and Cao M** (2015) Carbon nanotube-CdS core–shell nanowires with tunable and high-efficiency microwave absorption at elevated temperature. *Nanotechnology* **27**, 065702.
19. **Lu M-M, Cao M-S, Chen Y-H, Cao W-Q, Liu J, Shi H-L, Zhang D-Q, Wang W-Z and Yuan J** (2015) Multiscale assembly of grape-like ferroferric oxide and carbon nanotubes: a smart absorber prototype varying temperature to tune intensities. *ACS Applied Materials & Interfaces* **7**, 19408–19415.
20. **Yang Q, Liu L, Hui D and Chipara M** (2016) Microstructure, electrical conductivity and microwave absorption properties of γ-FeNi decorated carbon nanotube composites. *Composites Part B: Engineering* **87**, 256–262.
21. **Shahzad F, Yu S, Kumar P, Lee J-W, Kim Y-H, Hong SM and Koo CM** (2015) Sulfur doped graphene/polystyrene nanocomposites for electromagnetic interference shielding. *Composite Structures* **133**, 1267–1275.
22. **Pitman KC, Lindley MW, Simkin D and Cooper JF** (1991) Radar absorbers: better by design. *IEE Proceedings F (Radar and Signal Processing)* **138**, 223–228.
23. **Spada LL and Vegni L** (2016) Metamaterial-based wideband electromagnetic wave absorber. *Optics Express* **24**, 5763–5772.
24. **Seng LY, Wee FH, Rahim HA, AbdulMalek M, You YK, Liyana Z and Ezanuddin AAM** (2016) Design of multiple-layer microwave absorbing structure based on rice husk and carbon nanotubes. *Applied Physics A* **123**, 73.
25. **Fante RL and McCormack MT** (1988) Reflection properties of the Salisbury screen. *IEEE Transactions on Antennas and Propagation* **36**, 1443–1454.
26. **Kazemzadeh A** (2011) Nonmagnetic ultrawideband absorber with optimal thickness. *IEEE Transactions on Antennas and Propagation* **59**, 135–140.
27. **Kubo O, Ido T and Yokoyama H** (1982) Properties of Ba ferrite particles for perpendicular magnetic recording media. *IEEE Transactions on Magnetics* **18**, 1122–1124.
28. **Batrakov K, Kuzhir P, Maksimenko S, Paddubskaya A, Voronovich S, Lambin P, Kaplas T and Svirko Y** (2014) Flexible transparent graphene/polymer multilayers for efficient electromagnetic field absorption. *Scientific Reports* **4**, 7191.
29. **Zhi Cheng Y, Wang Y, Nie Y, Zhou Gong R, Xiong X and Wang X** (2012) Design, fabrication and measurement of a broadband polarization-insensitive metamaterial absorber based on lumped elements. *Journal of Applied Physics* **111**, 044902.
30. **Sun J, Liu L, Dong G and Zhou J** (2011) An extremely broad band metamaterial absorber based on destructive interference. *Optics Express* **19**, 21155–21162.
31. **Rotshild D, Azoulay Y, Ochana M, Shulzinger A and Abramovich A** (2015) Real time detection and recognition of micro-poisons in aqueous solutions and atmosphere using perfect absorber metamaterial in millimeter wavelength regime. *2015 IEEE International Conference on Microwaves, Communications, Antennas and Electronic Systems (COMCAS)*, pp. 1–4. https://doi.org/10.1109/COMCAS.2015.7360466.
32. **Li L and Lv Z** (2017) Ultra-wideband polarization-insensitive and wide-angle thin absorber based on resistive metasurfaces with three resonant modes. *Journal of Applied Physics* **122**, 055104.
33. **Yin Z, Lu Y, Gao S, Yang J, Lai W, Li Z and Deng G** (2019) Optically transparent and single-band metamaterial absorber based on indium-tin-oxide. *International Journal of RF and Microwave Computer-Aided Engineering* **29**, e21536.
34. **Lai S, Wu Y, Wang J, Wu W and Gu W** (2018) Optical-transparent flexible broadband absorbers based on the ITO–PET–ITO structure. *Optical Materials Express* **8**, 1585–1592.
35. **Zhang C, Yang J, Cao W, Yuan W, Ke J, Yang L, Cheng Q and Cui T** (2019) Transparently curved metamaterial with broadband millimeter wave absorption. *Photonics Research* **7**, 478–485.
36. **Lai S, Wu Y, Zhu X, Gu W and Wu W** (2017) An optically transparent ultrabroadband microwave absorber. *IEEE Photonics Journal* **9**, 1–10.
37. **Takizawa K and Hashimoto O** (1999) Transparent wave absorber using resistive thin film at V-band frequency. *IEEE Transactions on Microwave Theory and Techniques* **47**, 1137–1141.
38. **Narayan S, Latha S and Jha R** (2013) EM Analysis of Metamaterial Based Radar Absorbing Structure (RAS) for Millimeter Wave Applications. (2013)/paper/EM-Analysis-of-Metamaterial-Based-Radar-(RAS)-for-Narayan-Latha/24bfb8cae23013361445941fe274efb8e5259476 (accessed September 13, 2020).

https://doi.org/10.1017/S1759078722000162 Published online by Cambridge University Press

39. **Sakran F, Neve-Oz Y, Ron A, Golosovsky M, Davidov D and Frenkel A** (2008) Absorbing frequency-selective-surface for the mm-wave range. *IEEE Transactions on Antennas and Propagation* **56**, 2649–2655.
40. **Anwar RS, Mao L and Ning H** (2018) Frequency selective surfaces: a review. *Applied Sciences* **8**, 1689.
41. **Lozitsky OV, Vovchenko LL, Matzui LY, Oliynyk VV and Zagorodnii VV** (2020) Microwave properties of epoxy composites with mixed filler carbon nanotubes/$BaTiO_3$. *Applied Nanoscience* **10**, 2759–2767.
42. **Xiao D, Zhu M, Wang Q, Sun L, Zhao C, Ng ZK, Teo EHT, Hu F and Tu L** (2020) A flexible and ultra-broadband terahertz wave absorber based on graphene–vertically aligned carbon nanotube hybrids. *Journal of Materials Chemistry C* **8**, 7244–7252.
43. **Quiévy N, Bollen P, Thomassin J-M, Detrembleur C, Pardoen T, Bailly C and Huynen I** (2012) Electromagnetic absorption properties of carbon nanotube nanocomposite foam filling honeycomb waveguide structures. *IEEE Transactions on Electromagnetic Compatibility* **54**, 43–51.
44. **Danlée Y, Bailly C and Huynen I** (2017) Flexible polarization-dependent absorbers based on patterned carbon nanotubes films. *Microwave and Optical Technology Letters* **59**, 1164–1167.
45. **Anoshkin IV, Campion J, Lioubtchenko DV and Oberhammer J** (2018) Freeze-dried carbon nanotube aerogels for high-frequency absorber applications. *ACS Applied Materials & Interfaces* **10**, 19806–19811.
46. **Gui X, Wang K, Wei J, Lü R, Shu Q, Jia Y, Wang C, Zhu H and Wu D** (2009) Microwave absorbing properties and magnetic properties of different carbon nanotubes. *Science in China Series E: Technological Sciences* **52**, 227–231.
47. **Liu T and Kim S-S** (2018) Ultrawide bandwidth electromagnetic wave absorbers composed of double-layer frequency selective surfaces with different patterns. *Scientific Reports* **8**, 13889.
48. **Tang J, Xiao Z, Xu K, Ma X and Wang Z** (2016) Polarization-controlled metamaterial absorber with extremely bandwidth and wide incidence angle. *Plasmonics* **11**, 1393–1399.
49. **Ling X, Xiao Z, Zheng X, Tang J and Xu K** (2016) Ultra-broadband metamaterial absorber based on the structure of resistive films. *Journal of Electromagnetic Waves and Applications* **30**, 2325–2333.
50. **Chambers B and Tennant A** (1996) Optimised design of Jaumann radar absorbing materials using a genetic algorithm. *IEE Proceedings – Radar, Sonar and Navigation* **143**, 23–30.
51. **Du Toit LJ** (1994) The design of Jauman absorbers. *IEEE Antennas and Propagation Magazine* **36**, 17–25.
52. **Singh PK, Korolev KA, Afsar MN and Sonkusale S** (2011) Single and dual band 77/95/110 GHz metamaterial absorbers on flexible polyimide substrate. *Applied Physics Letters* **99**, 264101.
53. **Singh P, Kabiri Ameri S, Chao L, Afsar MN and Sonkusale S** (2013) Broadband millimeterwave metamaterial absorber based on embedding of dual resonators. *Progress in Electromagnetics Research* **142**, 625–638.
54. **Lee D, Sung H-K and Lim S** (2016) Flexible subterahertz metamaterial absorber fabrication using inkjet printing technology. *Applied Physics B* **122**, 206.
55. **Liu T and Kim S-S** (2019) Ultrawide bandwidth electromagnetic wave absorbers using a high-capacitive folded spiral frequency selective surface in a multilayer structure. *Scientific Reports* **9**, 16494.
56. **Ghosh S, Bhattacharyya S and Srivastava KV** (2016) Design, characterisation and fabrication of a broadband polarisation-insensitive multilayer circuit analogue absorber. IET Microwaves, *Antennas and Propagation* **10**, 850–855.
57. **Han Y, Che W, Christopoulos C, Xiong Y and Chang Y** (2016) A fast and efficient design method for circuit analog absorbers consisting of resistive square-loop arrays. *IEEE Transactions on Electromagnetic Compatibility* **58**, 747–757.
58. **Yang G-H, Liu X-X, Lv Y-L, Fu J-H, Wu Q and Gu X** (2014) Broadband polarization-insensitive absorber based on gradient structure metamaterial. *Journal of Applied Physics* **115**, 17E523.
59. **Yoo M and Lim S** (2014) Polarization-independent and ultrawideband metamaterial absorber using a hexagonal artificial impedance surface and a resistor-capacitor layer. *IEEE Transactions on Antennas and Propagation* **62**, 2652–2658.
60. **Chen J, Hu Z, Wang G, Huang X, Wang S, Hu X and Liu M** (2015) High-impedance surface-based broadband absorbers With interference theory. *IEEE Transactions on Antennas and Propagation* **63**, 4367–4374.
61. **Zhang H-B, Zhou P-H, Lu H-P, Xu Y-Q, Liang D-F and Deng L-J** (2013) Resistance selection of high impedance surface absorbers for perfect and broadband absorption. *IEEE Transactions on Antennas and Propagation* **61**, 76–979.
62. **Sun L, Cheng H, Zhou Y and Wang J** (2012) Broadband metamaterial absorber based on coupling resistive frequency selective surface. *Optics Express* **20**, 4675–4680.
63. **Li M, Xiao S, Bai Y-Y and Wang B-Z** (2012) An ultrathin and broadband radar absorber using resistive FSS. *IEEE Antennas and Wireless Propagation Letters* **11**, 748–751.
64. **Olszewska-Placha M, Salski B, Janczak D, Bajurko PR, Gwarek W and Jakubowska M** (2015) A broadband absorber with a resistive pattern made of Ink with graphene nano-platelets. *IEEE Transactions on Antennas and Propagation* **63**, 565–572.
65. **Costa F, Monorchio A and Manara G** (2010) Analysis and design of ultra thin electromagnetic absorbers comprising resistively loaded high impedance surfaces. *IEEE Transactions on Antennas and Propagation* **58**, 1551–1558.
66. **Yin X, Long C, Li J, Zhu H, Chen L, Guan J and Li X** (2015) Ultra-wideband microwave absorber by connecting multiple absorption bands of two different-sized hyperbolic metamaterial waveguide arrays. *Scientific Reports* **5**, 1–8.
67. **Zhang T, Chen L and Li X** (2013) Graphene-based tunable broadband hyperlens for far-field subdiffraction imaging at mid-infrared frequencies. *Optics Express* **21**, 20888–20899.
68. **Yang X, Yao J, Rho J, Yin X and Zhang X** (2012) Experimental realization of three-dimensional indefinite cavities at the nanoscale with anomalous scaling laws. *Nature Photonics* **6**, 450–454.
69. **Krishnamoorthy HNS, Jacob Z, Narimanov E, Kretzschmar I and Menon VM** (2012) Topological transitions in metamaterials. *Science* **336**, 205–209.
70. **Jacob Z, Alekseyev LV and Narimanov E** (2006) Optical hyperlens: far-field imaging beyond the diffraction limit. *Optics Express* **14**, 8247–8256.
71. **Chen L and Wang GP** (2009) Pyramid-shaped hyperlenses for three-dimensional subdiffraction optical imaging. *Optics Express* **17**, 3903–3912.
72. **Salandrino A and Engheta N** (2006) Far-field subdiffraction optical microscopy using metamaterial crystals: theory and simulations. *Physical Review B* **74**, 075103.
73. **Li W, Wu T, Wang W, Zhai P and Guan J** (2014) Broadband patterned magnetic microwave absorber. *Journal of Applied Physics* **116**, 044110.
74. **Yahiaoui R, Tan S, Cong L, Singh R, Yan F and Zhang W** (2015) Multispectral terahertz sensing with highly flexible ultrathin metamaterial absorber. *Journal of Applied Physics* **118**, 083103.
75. **Zhou Z, Chen K, Zhao J, Chen P, Jiang T, Zhu B, Feng Y and Li Y** (2017) Metasurface Salisbury screen: achieving ultra-wideband microwave absorption. *Optics Express* **25**, 30241–30252.
76. **Soh T, Kondo A, Toyota M and Hashimoto O** (2003) A basic study of millimeter-wave absorber for two frequency bands using transparent resistive films. *2003 IEEE Symposium on Electromagnetic Compatibility. Symposium Record (Cat. No. 03CH37446)*, pp. 149–154 vol. **1**. https://doi.org/10.1109/ISEMC.2003.1236581.
77. **Lu Y, Chi B, Liu D, Gao S, Gao P, Huang Y, Yang J, Yin Z and Deng G** (2018) Wideband metamaterial absorbers based on conductive plastic with additive manufacturing technology. *ACS Omega* **3**, 11144–11150.
78. **Wu Y, Fu C, Qian S, Zong Z, Wu X, Yue Y and Gu W** (2020) Flexible and transparent W-band absorber fabricated by EHD printing technology. *IEEE Antennas and Wireless Propagation Letters* **19**, 1345–1349. tps://doi.org/10.1109/LAWP.2020.3000786.
79. **Tang J, Xiao Z, Xu K and Liu D** (2016) A polarization insensitive and broadband metamaterial absorber based on three-dimensional structure. *Optics Communications* **372**, 64–70.

https://doi.org/10.1017/S1759078722000162 Published online by Cambridge University Press

80. **Vahidi A, Rajabalipanah H, Abdolali A and Cheldavi A** (2018) A honeycomb-like three-dimensional metamaterial absorber via super-wideband and wide-angle performances at millimeter wave and low THz frequencies. *Applied Physics A* **124**, 337.
81. **Petroff M, Appel J, Rostem K, Bennett CL, Eimer J, Marriage T, Ramirez J and Wollack EJ** (2019) A 3D-printed broadband millimeter wave absorber. *Review of Scientific Instruments* **90**, 024701.
82. **Adachi S, Hattori M, Kanno F, Kiuchi K, Okada T and Tajima O** (2020) Production method of millimeter-wave absorber with 3D-printed mold. *Review of Scientific Instruments* **91**, 016103.
83. **Rashid AK, Li B and Shen Z** (2014) An overview of three-dimensional frequency-selective structures. *IEEE Antennas and Propagation Magazine* **56**, 43–67.
84. **Hajizadegan M, Ahmadi V and Sakhdari M** (2013) Design and analysis of ultrafast and tunable all optical metamaterial switch enhanced by metal nanocomposite. *Journal of Lightwave Technology* **31**, 1877–1883.
85. **Li S-J, Gao J, Cao X-Y, Zhang Z, Liu T, Zheng Y-J, Zhang C and Zheng G** (2015) Hybrid metamaterial device with wideband absorption and multiband transmission based on spoof surface plasmon polaritons and perfect absorber. *Applied Physics Letters* **106**, 181103.
86. **Wu D, Liu Y, Yu Z, Chen L, Ma R, Li Y, Li R and Ye H** (2016) Wide-angle, polarization-insensitive and broadband absorber based on eight-fold symmetric SRRs metamaterial. *Optics Communications* **380**, 221–226.
87. **Sun H, Gu C, Chen X, Li Z, Liu L, Xu B and Zhou Z** (2017) Broadband and broad-angle polarization-independent metasurface for radar cross section reduction. *Scientific Reports* **7**, 40782.
88. **Xin W, Binzhen Z, Wanjun W, Junlin W and Junping D** (2017) Design and characterization of an ultrabroadband metamaterial microwave absorber. *IEEE Photonics Journal* **9**, 1–13.
89. **Wang LS, Xia DY, Ding XY and Wang Y** (2018) The design of wide-band metamaterial absorber at E band based on defect. *IOP Conference Series: Materials Science and Engineering* **292**, 012061.
90. **Deng G, Xia T, Yang J and Yin Z** (2018) Triple-band polarisation-independent metamaterial absorber at mm wave frequency band. *IET Microwaves, Antennas & Propagation* **12**, 1120–1125.
91. **Ahmad H, Khan MU, Tahir FA, Hussain R and Sharawi MS** (2018) Microwave absorber using single-layer FSS with wideband operation above the X-band. *12th European Conference on Antennas and Propagation (EuCAP 2018), London, UK*, **155** (3 pp.). https://doi.org/10.1049/cp.2018.0514.
92. **Wu Y, Deng Y, Wang J, Zong Z, Chen X and Gu W** (2019) THZ broadband absorber fabricated by EHD printing technology with high error tolerance. *IEEE Transactions on Terahertz Science and Technology* **9**, 637–642.
93. **Schnabel W** (2014) *Polymers and Electromagnetic Radiation: Fundamentals and Practical Applications*. Weinheim, Germany: John Wiley & Sons.
94. **Pitt C, Barth B and Godard B** (1957) Electrical properties of epoxy resins. *IRE Transactions on Component Parts* **4**, 110–113.
95. **Soh T, Yoshioka N and Hashimoto O** (1999) Millimeter wave absorber using epoxy-modified urethane rubber mixed with carbon particles at 60 GHz frequency band. *1999 International Symposium on Electromagnetic Compatibility (IEEE Cat. No. 99EX147) (1999)*, p. 788. https://doi.org/10.1109/ELMAGC.1999.801447.
96. **Soh T and Hashimoto O** (2000) Absorption characteristics in 50 to 110-GHz of 60-GHz wave absorber using epoxy-modified urethane rubber mixed with carbon particles. In *Proceedings of SPIE Vol. 4111: Terahertz and Gigahertz Electronics and Photonics II*. San Diego, CA: International Society for Optics and Photonics, pp. 227–231. https://doi.org/10.1117/12.422150.
97. **Soh T, Yoshioka N and Hashimoto O** (1999) A fundamental study of millimeter-wave absorbers composed of epoxy-modified urethane rubber mixed with carbon particles for 76 GHz or 94 GHz frequency band (undefined).
98. **Xiao B, Chen M, Hu R, Xu X, Deng X, Niu Y, Li X and Wang H** (2019) Epoxy-based ceramic-polymer composite with excellent millimeter-wave broadband absorption properties by Facile approach. *Advanced Engineering Materials* **21**, 1900981.
99. **Bellucci S, Micciulla F, Levin VM, Petronyuk YS, Chernozatonskii LA, Kuzhir PP, Paddubskaya AG, Macutkevic J, Pletnev MA, Fierro V and Celzard A** (2015) Microstructure, elastic and electromagnetic properties of epoxy-graphite composites. *AIP Advances* **5**, 067137.
100. **Suda Y, Matsuo R, Yoshii T, Yasudomi S, Tanimoto T, Harigai T, Takikawa H, Setaka T, Matsuda K, Suizu K, Shima H, Sandhu A and Sharma J** (2018) Electromagnetic wave absorption properties of carbon nanocoil composites in the millimeter waveband. *AIP Conference Proceedings*, 1929 (2018) 020021. https://doi.org/10.1063/1.5021934.
101. **Yang CC, Gung YJ, Shih CC, Hung WC and Wu KH** (2011) Synthesis, infrared and microwave absorbing properties of ($BaFe_{12}O_{19}$ + $BaTiO_3$)/polyaniline composite. *Journal of Magnetism and Magnetic Materials* **323**, 933–938.
102. **Pawar SP, Biswas S, Kar GP and Bose S** (2016) High frequency millimetre wave absorbers derived from polymeric nanocomposites. *Polymer* **84**, 398–419.
103. **Zhu D and Li E-P** (2015) A tunable wideband absorber based on periodic resistive patterned graphene. *2015 Asia-Pacific Microwave Conference (APMC)* (2015), pp. 1–3. https://doi.org/10.1109/APMC.2015.7412948.
104. **Zhang Y, Huang Y, Zhang T, Chang H, Xiao P, Chen H, Huang Z and Chen Y** (2015) Broadband and tunable high-performance microwave absorption of an ultralight and highly compressible graphene foam. *Advanced Materials* **27**, 2049–2053.
105. **Zhu D-K, Li Y-S, Yin W-Y and Li E-P** (2016) A transparent broadband absorber based on graphene. *2016 Asia-Pacific International Symposium on Electromagnetic Compatibility (APEMC)* (2016), pp. 1025–1027. https://doi.org/10.1109/APEMC.2016.7522935.
106. **Ma W, Chen H, Hou S, Huang Z, Huang Y, Xu S, Fan F and Chen Y** (2019) Compressible highly stable 3D porous MXene/GO foam with a tunable high-performance stealth property in the terahertz band. *ACS Applied Materials & Interfaces* **11**, 25369–25377.
107. **Sano E and Akiba E** (2014) Electromagnetic absorbing materials using nonwoven fabrics coated with multi-walled carbon nanotubes. *Carbon* **78**, 463–468.
108. **Nefedova II, Lioubtchenko DV, Nefedov IS and Räisänen AV** (2015) Dielectric constant estimation of a carbon nanotube layer on the dielectric Rod waveguide at millimeter wavelengths. *IEEE Transactions on Microwave Theory and Techniques* **63**, 3265–3271.
109. **Wu ZP, Cheng DM, Ma WJ, Hu JW, Yin YH, Hu YY, Li YS, Yang JG and Xu QF** (2015) Electromagnetic interference shielding effectiveness of composite carbon nanotube macro-film at a high frequency range of 40 GHz to 60 GHz. *AIP Advances* **5**, 067130.
110. **Dhawan SK, Singh N and Rodrigues D** (2003) Electromagnetic shielding behaviour of conducting polyaniline composites. *Science and Technology of Advanced Materials* **4**, 105–113.
111. **Xu F, Ma L, Gan M, Tang J, Li Z, Zheng J, Zhang J, Xie S, Yin H, Shen X, Hu J and Zhang F** (2014) Preparation and characterization of chiral polyaniline/barium hexaferrite composite with enhanced microwave absorbing properties. *Journal of Alloys and Compounds* **593**, 24–29.
112. **Ćirić-Marjanović G** (2013) Recent advances in polyaniline research: polymerization mechanisms, structural aspects, properties and applications. *Synthetic Metals* **177**, 1–47.
113. **Xuan X, Zhang HY, Zeng GX, Bo NK and Chan CH** (2016) Millimeter wave absorbing electromagnetic properties of ZnO whisker/silicon resin coating material. *Materials Science Forum* **852**, 1055–1059.
114. **Xu G, Zhang J, Zang X, Sugihara O, Zhao H and Cai B** (2016) 0.1–20 THz ultra-broadband perfect absorber via a flat multi-layer structure. *Optics Express* **24**, 23177–23185.
115. **Barani Z, Kargar F, Godziszewski K, Rehman A, Yashchyshyn Y, Rumyantsev S, Cywiński G, Knap W and Balandin AA** (2020) Graphene epoxy-based composites as efficient electromagnetic absorbers in the extremely high-frequency band. *ACS Applied Materials & Interfaces* **12**, 28635–28644.
116. **Batrakov K, Kuzhir P, Maksimenko S, Volynets N, Voronovich S, Paddubskaya A, Valusis G, Kaplas T, Svirko Y and Lambin P** (2016)

https://doi.org/10.1017/S1759078722000162 Published online by Cambridge University Press

Enhanced microwave-to-terahertz absorption in graphene. *Applied Physics Letters* **108**, 123101.
117. **Liu X, Yuan WT, Yuan Y, Wei WW and Yuan NC** (2018) A novel tunable broadband absorber based on graphene. *IOP Conference Series: Materials Science and Engineering* **382**, 022071.
118. **Hung W-C, Cheng K-F, Lan C-H, Chang Y-C and Wu K-H** (2016) Preparation and infrared/millimeter wave attenuation properties of magnetic expanded graphite by explosive combustion. *Materials Express* **6**, 53–60.
119. **Chen Y, Fu X, Liu L, Zhang Y, Cao L, Yuan D and Liu P** (2019) Millimeter wave absorbing property of flexible graphene/acrylonitrile-butadiene rubber composite in 5G frequency band. *Polymer-Plastics Technology and Materials* **58**, 903–914.
120. **Wu B, Tuncer HM, Naeem M, Yang B, Cole MT, Milne WI and Hao Y** (2014) Experimental demonstration of a transparent graphene millimetre wave absorber with 28% fractional bandwidth at 140 GHz. *Scientific Reports* **4**, 4130.
121. **Mencarelli D, Pierantoni L, Stocchi M and Bellucci S** (2016) Efficient and versatile graphene-based multilayers for EM field absorption. *Applied Physics Letters* **109**, 093103.
122. **Danlée Y, Huynen I and Bailly C** (2012) Thin smart multilayer microwave absorber based on hybrid structure of polymer and carbon nanotubes. *Applied Physics Letters* **100**, 213105.
123. **Biswas S, Panja SS and Bose S** (2017) Unique multilayered assembly consisting of "flower-like" ferrite nanoclusters conjugated with MWCNT as millimeter wave absorbers. *The Journal of Physical Chemistry C* **121**, 13998–14009.
124. **Hirose K and Ono T** (2016) Electromagnetic wave absorber, US9276326B2.
125. **Yu H-F and Huang K-C** (2003) Effects of pH and citric acid contents on characteristics of ester-derived $BaFe_{12}O_{19}$ powder. *Journal of Magnetism and Magnetic Materials* **260**, 455–461.
126. **Ting T-H and Wu K-H** (2010) Synthesis, characterization of polyaniline/$BaFe_{12}O_{19}$ composites with microwave-absorbing properties. *Journal of Magnetism and Magnetic Materials* **322**, 2160–2166.
127. **Gu H, Huang Y, Zhang X, Wang Q, Zhu J, Shao L, Haldolaarachchige N, Young DP, Wei S and Guo Z** (2012) Magnetoresistive polyaniline-magnetite nanocomposites with negative dielectrical properties. *Polymer* **53**, 801–809.
128. **Belaabed B, Wojkiewicz JL, Lamouri S, El Kamchi N and Lasri T** (2012) Synthesis and characterization of hybrid conducting composites based on polyaniline/magnetite fillers with improved microwave absorption properties. *Journal of Alloys and Compounds* **527**, 137–144.
129. **Xu F, Ma L, Huo Q, Gan M and Tang J** (2015) Microwave absorbing properties and structural design of microwave absorbers based on polyaniline and polyaniline/magnetite nanocomposite. *Journal of Magnetism and Magnetic Materials* **374**, 311–316.
130. **Wu KH, Ting TH, Wang GP, Yang CC and Tsai CW** (2008) Synthesis and microwave electromagnetic characteristics of bamboo charcoal/polyaniline composites in 2–40 GHz. *Synthetic Metals* **158**, 688–694.
131. **Xudong C, Jianjiang W, Baocai X, Hongfei L and Xingjian H** (n.d.). Research status in hollow microsphere: preparation methods and application. *Materials Review* 2012 年 19 期 **26**, 36–39. doi: http://en.cnki.com.cn/Article_en/CJFDTotal-CLDB201219010.htm.
132. **Zhang Y, Wang JM and Zhou TG** (2014) Effect of doping cerium oxide on microwave absorbing properties of polyaniline/Al-alloy foams composite materials. *Advanced Materials Research* **893**, 295–298.
133. **Yu Z** (2019) Effect of doping rare earth oxides on microwave absorbing properties of polyaniline/Al-alloy foams composite materials. *IOP Conference Series: Materials Science and Engineering* **612**, 032185.
134. **Kamei T, Shima H, Yamamoto T, Ogino S and Ishii S** (2017) Millimeter-wave absorption properties of thin wave absorber in free space with new porous carbon material. *Wireless Engineering and Technology* **8**, 51–58.
135. **Liu JR, Itoh M, Horikawa T, Machida K, Sugimoto S and Maeda T** (2005) Gigahertz range electromagnetic wave absorbers made of amorphous-carbon-based magnetic nanocomposites. *Journal of Applied Physics* **98**, 054305.
136. **Letellier M, Macutkevic J, Paddubskaya A, Plyushch A, Kuzhir P, Ivanov M, Banys J, Pizzi A, Fierro V and Celzard A** (2015) Tannin-based carbon foams for electromagnetic applications. *IEEE Transactions on Electromagnetic Compatibility* **57**, 989–995.
137. **Sen G, Islam SN, Banerjee A and Das S** (2017) Broadband perfect metamaterial absorber on thin substrate for X-band and Ku-band applications. *Progress in Electromagnetics Research* **73**, 9–16.
138. **Lee D, Kim HK and Lim S** (2017) Textile metamaterial absorber using screen printed channel logo. *Microwave and Optical Technology Letters* **59**, 1424–1427.
139. **Asadchy VS, Faniayeu IA, Ra'di Y, Khakhomov SA, Semchenko IV and Tretyakov SA** (2015) Broadband reflectionless metasheets: frequency-selective transmission and perfect absorption. *Physical Review X* **5**, 031005.
140. **Hamm JM, Wuestner S, Tsakmakidis KL and Hess O** (2011) Theory of light amplification in active fishnet metamaterials. *Physical Review Letters* **107**, 167405.
141. **Assimonis SD and Fusco V** (2019) Polarization insensitive, wide-angle, ultra-wideband, flexible, resistively loaded, electromagnetic metamaterial absorber using conventional inkjet-printing technology. *Scientific Reports* **9**, 12334.



Anupriya Choudhary currently works as a Ph.D. scholar in Electronics and Communications Engineering department at BIT Mesra, Ranchi. She has obtained her M.Tech. from BIT Mesra in Nanoscience and Nanotechnology in 2017. She has completed her B.Tech. from Electronics and Communications Engineering department at MIT Manipal, Karnataka in 2015. Her research interests include absorbers, selective surfaces (FSSs), and materials' metamaterials, frequency characterization.



Srikanta Pal received his B.Tech. from NIT Warangal. He received his M.E. degree from Jadavpur University and his D.PHIL. from Oxford University. He is currently working as a professor in the ECE department at BIT Mesra, Ranchi. He has 8 years of experience in the industry and 22 years in research around the globe. He has teaching experience of more than 15 years. His research interest includes antennas, filter synthesis and analysis, metamaterials, microwave/terahertz imaging and sensors, statistical signal processing, radio astronomy, fractals, EBG/PBG, DGS, reconfigurable geometries and frequency selective surfaces (FSSs), computational electromagnetics, thin film-based wireless components using high-temperature superconductors, ferroelectrics, etc.



Gautam Sarkhel is currently the Head of Department and Professor of Chemical Engineering Department, BIT Mesra. He completed his B.Tech. in 1998 from Calcutta University. Thereafter, he completed his M.Tech. from IIT Delhi in 1999 and his Ph.D. from Jadavpur University in 2006. He has more than 19 years of teaching and research experience at BIT Mesra, Ranchi. His research interests include polymer composites, surface coating, membrane science and technology, reactive polymer blends, specialty polymers and membranes for fuel cells, etc.

https://doi.org/10.1017/S1759078722000162 Published online by Cambridge University Press